nature research

Peer Review File

Manuscript Title: Giant nonlinear optical responses from photon avalanching nanoparticles

Editorial Notes:

Reviewer Comments & Author Rebuttals

Reviewer Reports on the Initial Version:

Referee #1 (Remarks to the Author):

[see also attached pdf]

Referee report on 'Giant nonlinear optical response from photon avalanching nanoparticles' by Changhwan Lee et al.

The manuscript describes important and impressive results on the observation and application of photon avalanching (PA) in Tm3+ doped NaYF4 core-shell nanoparticles (NPs). The work is convincingly presented: the steep power dependence and the long onset times just above the pumping threshold are clear signatures of the PA phenomenon and beautifully demonstrate that the observed effect results from a true photon avalanche in the Tm-doped NPs. The work is expected to have a large impact. Various research areas where the extreme non-linearity can be used are mentioned and one (high resolution confocal imaging) is shown to work. The demonstration of a spatial resolution around 70 nm is impressive and indeed much simpler to achieve than with other methods that are presently used to beat the diffraction limit. Based on this assessment, I support publication of this work in Nature.

There are some questions that should be addressed or clarified before publication. The various points I found appear mostly 'chronologically' (in the order the appear in the manuscript) or, where appropriate, by jumping to related sections in the Supplementary Materials. None of the issues are too serious as they do not affect the validity of the main results and conclusions of the manuscript.

1 Abstract – In the abstract it is mentioned that the avalanching NPs can be pumped with continuous wave or pulsed lasers. This initially confused me, as PA is a process observed for CW pumping (and cannot be excited with a laser pulse as it relies on building up population in the intermediate level during CW excitation). In the supporting information it became clear that some experiments (1450 nm excitation) were done with a pulsed 80 MHz femtosecond OPO laser. For the present experiments this is analogous to CW excitation as all effects take place on much longer timescales than the 12 ns intervals between the 200 fs pulses of the OPO. In their conclusions the authors seem to realize this and indicate 'realizing PA in engineered nanocrystals at room temperature with continuous wave pumping'. No mention of pulsed excitation there. I suggest to also leave 'pulsed lasers' out in the Abstract.

2 Figure 1 – The length of the arrows represents the energy of the photons and this is mostly correct. However, for the green arrows, representing the cross-relaxation process, one arrow is longer than the other as the 3H4-3F4 energy difference is larger than the 3H6-3F4 energy difference. This makes the cross-relaxation process phonon assisted. My suggestion is to adapt the length to make them the same and use the curvy light grey arrow to make clear that phonon emission is involved (similar to the way other phonon relaxation processes are shown in Figure 1). The need for phonon-assistance to make up for the ~1200 cm-1 energy mismatch is not really addressed in the manuscript - it is not unimportant as it may help in e.g. understanding differences in the dynamics in comparison with Tm3+ in other hosts with higher phonon frequencies (such as YAG).

3 Figure 1 – W2 and W3 are mentioned to be the 3F4 and 3H4 decay rates. Here, and elsewhere in

the manuscript it would be good to be more specific and define already in the beginning what is meant with decay rate. For the 3F4 level W2 is the sum of the radiative and non-radiative decay rates (W2R + W2NR). For the 3H4 level the decay rates include radiative and non-radiative decay from the 3H4 level as well as the strongly concentration dependent cross-relaxation rate s31 which is not included in W3 but considered separately. It would be good if this could be more clearly outlined.

4 Figure 1 – small detail: include 'concentration' after Tm3+ in Tm3+ > 8%.

5 At several places the non-resonant GSA is mentioned. For people unfamiliar with lanthanide spectroscopy this may be puzzling as non-resonant excitation is not possible (apart from some fancy spectroscopy experiments driving transitions slightly off resonance, e.g. to observe changes in the Rabi frequency). In fact the excitation here is resonant, but with a weakly absorbing vibronic overtone. I noticed that the excitation is chosen to be about 1500 cm-1 above the resonant level (3F4 for the 1450 nm excitation and 3H5 for the 1064 nm excitation). I assume this was chosen deliberately to excite (resonantly) in the very weak 3rd or 4th vibrational overtone of the 3H4-3F4 or 3H4-3H5 electronic transitions. Vibronic coupling is extremely weak for lanthanides which makes the oscillator strengths of these 'non-resonant' excitations very small, indeed some 104 times weaker than excitation resonant with the purely electronic f-f transitions. It would be helpful to briefly explain the origin of the 'non-resonant' excitation and the background of the 104 ratio of ESA-to-GSA.

6 Figure 2 concerns measurements of a thin film of drop casted NPs, providing an ensemble result. At other places in the manuscript and Supplementary Materials it is not always clear if it concerns single NP measurements or ensemble NP measurements. I assume Figs 2 and 3 in the main text and Figs S3, S4 all concern ensemble measurements on nanoparticle films. In Fig S7 this is clearly indicated. A short mention of this would be helpful. It could be interesting to study differences between individual (single) nanoparticles from the same batch which are expected to show different onset behavior depending on the variations of non-radiative processes in NPs with less/more defects, better/worse passivating shell.

7 The modelling is done using a model developed by Guy and Joubert for microcrystalline materials. Qualitatively, the results are consistent and the trends observed upon decreasing the W2NR rates by growing thicker shells and/or making bigger cores are in line with the expectations, shifting the threshold for PA to lower powers with decreasing W2NR. Quantitatively, the modelling is not clearly explained and assumptions are made that seem not correct. The Supporting Materials do not really help. It would be helpful to describe the procedure more clearly and be consistent. For example:

• s31 in the Main Text seems to be s3 in Supp Mat,

• The branching ratio b32 is (I assume, it is not explained) the radiative decay from 3H4 to 3F4, feeding the 3F4 level. The role of the 3H5 level is not clear. From the 3H5 level, there will be fast relaxation to the 3F4, also feeding 'level 2'. Is radiative decay from 3H4 to 3H5 included in b23?

• Table S3 has as a header 'Judd-Ofelt parameters and reduced matrix elements'. It would be wonderful to include these parameters (Judd-Ofelt parameters Ω2, Ω4 and Ω6 and reduced matrix elements U(2), U(4) and U(6) for all relevant transitions) since then we could calculate the branching ratio b23, the absorption cross section σESA, W2R, W3R etc. However, the table does not contain these parameters, but rather contains some numbers that seem to have been calculated from these parameters that were taken from data on Na0.4Y0.6F2.2:Tm3+ crystals. In a revised version it would be helpful to provide the Judd-Ofelt parameters and reduced matrix elements used, as well as a justification that the numbers for Na0.4Y0.6F2.2:Tm3+ are also valid for β-NaYF4:Tm3+. Did the authors check if σESA calculated with these Judd-Ofelt parameters matches the 5.6x10-25 m2 found here for the 3F4-3H4 transition??

• W3NR is taken as a constant and is (it seems) determined from the non-radiative multi-phonon relaxation rate in the microcrystalline Na0.4Y0.6F2.2:Tm3+ material. W2NR is not taken from this reference but fitted from the curves and found to vary and increase when non-radiative channels become more prominent in samples with smaller nanocrystal cores, thinner shells or higher doping concentrations. This variation is consistent with what is expected and indeed this changes the threshold for the PA effect in a logical manner. However, keeping W3NR constant seems not logical. Would the same variation in non-radiative decay found for W2NR due to surface defects

and phonon assistance not also be true for W3NR? The energy gaps for non-radiative decay W2NR (3F4-3H6, ~5000 cm-1) and W3NR (3H4-3H5, also ~5000 cm-1) are similar. At least, it should be mentioned why W2NR is assumed to vary while W3NR is taken as constant with a short explanation why this is allowed.
• It would have been good if changes in the changes in W2 that were extracted from the data in Fig. 3(a) were independently verified by luminescence decay measurements of the 3F4 emission under pulsed excitation.

8 The paper sometimes requires more effort than necessary to understand. In the main text sample variation is discussed for three different types of 8% Tm3+ samples. The results are in line with what is expected (thicker shell/larger particles results in a lower PA threshold because of less non-radiative losses W2NR). However, in Figure 3b there also seems to be a second type of 20% sample. This is used to determine the slope differences in that depend on s31. Besides my feeling that these slope differences in Fig. 3b are not really convincing, I wondered what the second 20% sample was. I could not find it in the main text. The Supp Mat shows indeed two different 20% NPs: Sample 6 and Sample 7 with a 17.5 nm core (sample no. 6) and a 10.4 nm core (sample no. 7) with the same 2.6/2.7 nm shell thickness. In Figure S3 it is shown that they have a different onset of the PA effect (note the x-axis in Figure S3 is not given in kW cm-2 as in all other power dependence Figures but in W/cm2). It is however not indicated which curve belongs to sample 6 and which to sample 7. Table S5 may provide the answer: in Table S5 the 'phonon assisted non-radiative relaxation rates' W2NR are given for Particle No. 2 to 8 (maybe change Particle No. to Sample No?). Surprisingly, W2NR is lower for the smaller core sample 7 (513 s-1) than for the larger core particle sample 6 (878 s-1). Is the lower PA threshold in Figure S3 for the smaller particle 7? This would be consistent with the lower W2NR but unexpected as smaller core NPs are expected to have higher non-radiative decay (as observed for the 8% NPs). It is unfortunate that discussion on the two 20% samples is missing, especially since the trend seems opposite to what is expected and what was observed for the 8% samples. In Table S6 the second 20% sample is missing again. It would be nice to see and compare the Δav values for the two 20% Tm3+ samples with different core sizes.
9 Table S5 shows that W2NR rate for sample 5 is 0. This seems to be very low. It deserves some discussion. The very thick shell of sample 5 may completely suppress quenching.
10 In Table S2 the core sizes for the elliptical particles are given for four samples which are the same as in Table S1 but now the numbers are given for the two axes which are used to determine the average diameter. For sample 1 this makes sense: (major axis + minor axis)/2 = (17.3+14.3)/2 = 15.8 nm – indeed the number in the column average and in Table S1. For sample 4, there is a 0.1 nm deviation – not a real problem. However, the number for the average (15.9 nm) is not the same as the number for sample 4 in Table S1 (17.3 nm). The numbers in Table S2 for samples 5 and 6 do not make sense at all, the minor axes are 4.0 and 3.0 nm – much too small, the average diameter for sample 6 (17.5 nm) is larger than that of the major axis (15.8 nm). Something seems to have gone wrong in Table S3– or I am missing something?
11 In line 178 it is mentioned that the quantum yield (QY) can exceed 20% for a pump power exceeding 105 W/cm2. In Figure 3c the QY is seen to exceed 40% and come very close to the theoretical maximum of 50%. Is the quantum yield defined as (number of 800 nm photons emitted)/(number of 1064 nm photons absorbed)? It will be good to mention 40% (and not 20%) if Figure 3c is correct and to clearly define quantum yield.

I realize the number of comments is somewhat high considering the excellent quality of the work and my positive recommendation for publication. It is however good for important results as presented here to explain all aspects clearly and help readers to easily understand figures without having to put in too much effort. Also, it is important to make it possible to understand and reproduce the fitting/analyses by providing more details, such as the values used for the Judd-Ofelt parameters and reduced matrix elements in the Supp. Mat.
My comments do not distract from the importance of a convincing demonstration of the strongly non-linear optical response in Tm3+-doped NPs. The origin is clearly identified as a photon avalanche effect and this is a breakthrough in the field. The potential impact is illustrated with

confocal imaging experiments showing how the PA effect can serve to easily obtain spatial resolutions well below the diffraction limit. In the future the extreme non-linearity in these and other NPs showing photon avalanche effects may be used for other applications. As noted in the introductory paragraph, I therefore recommend publication in Nature and hope my remarks will be considered as helpful.

ATTACHED PDF

Referee report on 'Giant nonlinear optical response from photon avalanching nanoparticles' by Changhwan Lee et al. The manuscript describes important and impressive results on the observation and application of photon avalanching (PA) in Tm3+ doped NaYF4 core-shell nanoparticles (NPs). The work is convincingly presented: the steep power dependence and the long onset times just above the pumping threshold are clear signatures of the PA phenomenon and beautifully demonstrate that the observed effect results from a true photon avalanche in the Tm-doped NPs. The work is expected to have a large impact. Various research areas where the extreme non-linearity can be used are mentioned and one (high resolution confocal imaging) is shown to work. The demonstration of a spatial resolution around 70 nm is impressive and indeed much simpler to achieve than with other methods that are presently used to beat the diffraction limit. Based on this assessment, I support publication of this work in Nature. There are some questions that should be addressed or clarified before publication. The various points I found appear mostly 'chronologically' (in the order the appear in the manuscript) or, where appropriate, by jumping to related sections in the Supplementary Materials. None of the issues are too serious as they do not affect the validity of the main results and conclusions of the manuscript. 1 Abstract – In the abstract it is mentioned that the avalanching NPs can be pumped with continuous wave or pulsed lasers. This initially confused me, as PA is a process observed for CW pumping (and cannot be excited with a laser pulse as it relies on building up population in the intermediate level during CW excitation). In the supporting information it became clear that some experiments (1450 nm excitation) were done with a pulsed 80 MHz femtosecond OPO laser. For the present experiments this is analogous to CW excitation as all effects take place on much longer timescales than the 12 ns intervals between the 200 fs pulses of the OPO. In their conclusions the authors seem to realize this and indicate 'realizing PA in engineered nanocrystals at room temperature with continuous wave pumping'. No mention of pulsed excitation there. I suggest to also leave 'pulsed lasers' out in the Abstract. 2 Figure 1 – The length of the arrows represents the energy of the photons and this is mostly correct. However, for the green arrows, representing the cross-relaxation process, one arrow is longer than the other as the 3H4- 3F4 energy difference is larger than the 3H6- 3F4 energy difference. This makes the cross-relaxation process phonon assisted. My suggestion is to adapt the length to make them the same and use the curvy light grey arrow to make clear that phonon emission is involved (similar to the way other phonon relaxation processes are shown in Figure 1). The need for phonon-assistance to make up for the ~1200 cm-1 energy mismatch is not really addressed in the manuscript - it is not unimportant as it may help in e.g. understanding differences in the dynamics in comparison with Tm3+ in other hosts with higher phonon frequencies (such as YAG). 3 Figure 1 – W2 and W3 are mentioned to be the 3F4 and 3H4 decay rates. Here, and elsewhere in the manuscript it would be good to be more specific and define already in the beginning what is meant with decay rate. For the 3F4 level W2 is the sum of the radiative and nonradiative decay rates (W2 R + W2 NR). For the 3H4 level the decay rates include radiative and non-radiative decay from the 3H4 level as well as the strongly concentration dependent crossrelaxation rate s31 which is not included in W3 but

considered separately. It would be good if this could be more clearly outlined. 4 Figure 1 – small detail: include 'concentration' after Tm3+ in Tm3+ > 8%. 5 At several places the non-resonant GSA is mentioned. For people unfamiliar with lanthanide spectroscopy this may be puzzling as non-resonant excitation is not possible (apart from some fancy spectroscopy experiments driving transitions slightly off resonance, e.g. to observe changes in the Rabi frequency). In fact the excitation here is resonant, but with a weakly absorbing vibronic overtone. I noticed that the excitation is chosen to be about 1500 cm-1 above the resonant level (3F4 for the 1450 nm excitation and 3H5 for the 1064 nm excitation). I assume this was chosen deliberately to excite (resonantly) in the very weak 3 rd or 4th vibrational overtone of the 3H4- 3F4 or 3H4- 3H5 electronic transitions. Vibronic coupling is extremely weak for lanthanides which makes the oscillator strengths of these 'non-resonant' excitations very small, indeed some 104 times weaker than excitation resonant with the purely electronic f-f transitions. It would be helpful to briefly explain the origin of the 'non-resonant' excitation and the background of the 104 ratio of ESA-to-GSA. 6 Figure 2 concerns measurements of a thin film of drop casted NPs, providing an ensemble result. At other places in the manuscript and Supplementary Materials it is not always clear if it concerns single NP measurements or ensemble NP measurements. I assume Figs 2 and 3 in the main text and Figs S3, S4 all concern ensemble measurements on nanoparticle films. In Fig S7 this is clearly indicated. A short mention of this would be helpful. It could be interesting to study differences between individual (single) nanoparticles from the same batch which are expected to show different onset behavior depending on the variations of non-radiative processes in NPs with less/more defects, better/worse passivating shell. 7 The modelling is done using a model developed by Guy and Joubert for microcrystalline materials. Qualitatively, the results are consistent and the trends observed upon decreasing the W2 NR rates by growing thicker shells and/or making bigger cores are in line with the expectations, shifting the threshold for PA to lower powers with decreasing W2 NR. Quantitatively, the modelling is not clearly explained and assumptions are made that seem not correct. The Supporting Materials do not really help. It would be helpful to describe the procedure more clearly and be consistent. For example: • s31 in the Main Text seems to be s3 in Supp Mat, • The branching ratio b32 is (I assume, it is not explained) the radiative decay from 3H4 to 3F4, feeding the 3F4 level. The role of the 3H5 level is not clear. From the 3H5 level, there will be fast relaxation to the 3F4, also feeding 'level 2'. Is radiative decay from 3H4 to 3H5 included in b23? • Table S3 has as a header 'Judd-Ofelt parameters and reduced matrix elements'. It would be wonderful to include these parameters (Judd-Ofelt parameters Ω2, Ω4 and Ω6 and reduced matrix elements U(2), U(4) and U(6) for all relevant transitions) since then we could calculate the branching ratio b23, the absorption cross section σESA, W2 R, W3 R etc. However, the table does not contain these parameters, but rather contains some numbers that seem to have been calculated from these parameters that were taken from data on Na0.4Y0.6F2.2:Tm3+ crystals. In a revised version it would be helpful to provide the Judd-Ofelt parameters and reduced matrix elements used, as well as a justification that the numbers for Na0.4Y0.6F2.2:Tm3+ are also valid for β-NaYF4:Tm3+. Did the authors check if σESA calculated with these Judd-Ofelt parameters matches the 5.6x10-25 m2 found here for the 3F4- 3H4 transition?? • W3 NR is taken as a constant and is (it seems) determined from the non-radiative multiphonon relaxation rate in the microcrystalline Na0.4Y0.6F2.2:Tm3+ material. W2 NR is not taken from this reference but fitted from the curves and found to vary and increase when non-radiative channels become more prominent in samples with smaller nanocrystal cores, thinner shells or higher doping concentrations. This variation is consistent with what is expected and indeed this changes the threshold for the PA effect in a logical manner. However, keeping W3 NR constant seems not logical.

Would the same variation in non-radiative decay found for W2 NR due to surface defects and phonon assistance not also be true for W3 NR? The energy gaps for non-radiative decay W2 NR (3F4- 3H6, ~5000 cm1) and W3 NR (3H4- 3H5, also ~5000 cm-1) are similar. At least, it should be mentioned why W2 NR is assumed to vary while W3 NR is taken as constant with a short explanation why this is allowed. • It would have been good if changes in the changes in W2 that were extracted from the data in Fig. 3(a) were independently verified by luminescence decay measurements of the 3F4 emission under pulsed excitation. 8 The paper sometimes requires more effort than necessary to understand. In the main text sample variation is discussed for three different types of 8% Tm3+ samples. The results are in line with what is expected (thicker shell/larger particles results in a lower PA threshold because of less non-radiative losses W2 NR). However, in Figure 3b there also seems to be a second type of 20% sample. This is used to determine the slope differences in that depend on s31. Besides my feeling that these slope differences in Fig. 3b are not really convincing, I wondered what the second 20% sample was. I could not find it in the main text. The Supp Mat shows indeed two different 20% NPs: Sample 6 and Sample 7 with a 17.5 nm core (sample no. 6) and a 10.4 nm core (sample no. 7) with the same 2.6/2.7 nm shell thickness. In Figure S3 it is shown that they have a different onset of the PA effect (note the x-axis in Figure S3 is not given in kW cm-2 as in all other power dependence Figures but in W/cm2). It is however not indicated which curve belongs to sample 6 and which to sample 7. Table S5 may provide the answer: in Table S5 the 'phonon assisted non-radiative relaxation rates' W2 NR are given for Particle No. 2 to 8 (maybe change Particle No. to Sample No?). Surprisingly, W2 NR is lower for the smaller core sample 7 (513 s-1) than for the larger core particle sample 6 (878 s-1). Is the lower PA threshold in Figure S3 for the smaller particle 7? This would be consistent with the lower W2 NR but unexpected as smaller core NPs are expected to have higher non-radiative decay (as observed for the 8% NPs). It is unfortunate that discussion on the two 20% samples is missing, especially since the trend seems opposite to what is expected and what was observed for the 8% samples. In Table S6 the second 20% sample is missing again. It would be nice to see and compare the Δav values for the two 20% Tm3+ samples with different core sizes. 9 Table S5 shows that W2 NR rate for sample 5 is 0. This seems to be very low. It deserves some discussion. The very thick shell of sample 5 may completely suppress quenching. 10 In Table S2 the core sizes for the elliptical particles are given for four samples which are the same as in Table S1 but now the numbers are given for the two axes which are used to determine the average diameter. For sample 1 this makes sense: (major axis + minor axis)/2 = (17.3+14.3)/2 = 15.8 nm – indeed the number in the column average and in Table S1. For sample 4, there is a 0.1 nm deviation – not a real problem. However, the number for the average (15.9 nm) is not the same as the number for sample 4 in Table S1 (17.3 nm). The numbers in Table S2 for samples 5 and 6 do not make sense at all, the minor axes are 4.0 and 3.0 nm – much too small, the average diameter for sample 6 (17.5 nm) is larger than that of the major axis (15.8 nm). Something seems to have gone wrong in Table S3– or I am missing something? 11 In line 178 it is mentioned that the quantum yield (QY) can exceed 20% for a pump power exceeding 105 W/cm2 . In Figure 3c the QY is seen to exceed 40% and come very close to the theoretical maximum of 50%. Is the quantum yield defined as (number of 800 nm photons emitted)/(number of 1064 nm photons absorbed)? It will be good to mention 40% (and not 20%) if Figure 3c is correct and to clearly define quantum yield. I realize the number of comments is somewhat high considering the excellent quality of the work and my positive recommendation for publication. It is however good for important results as presented here to explain all aspects clearly and help readers to easily understand figures without having to put in too much effort. Also, it is important to make it possible to understand and reproduce the fitting/analyses by providing more

details, such as the values used for the Judd-Ofelt parameters and reduced matrix elements in the Supp. Mat. My comments do not distract from the importance of a convincing demonstration of the strongly non-linear optical response in Tm3+-doped NPs. The origin is clearly identified as a photon avalanche effect and this is a breakthrough in the field. The potential impact is illustrated with confocal imaging experiments showing how the PA effect can serve to easily obtain spatial resolutions well below the diffraction limit. In the future the extreme non-linearity in these and other NPs showing photon avalanche effects may be used for other applications. As noted in the introductory paragraph, I therefore recommend publication in Nature and hope my remarks will be considered as helpful.

Referee #2 (Remarks to the Author):

In this manuscript, Schuck and co-workers reported a novel photon avalanching (PA) upconversion phenomenon at room temperature in heavily Tm3+ (>8 mol%) doped β-NaYF4 core/shell nanoparticles (NPs). The avalanching NPs (ANPs) can be pumped by either continuous-wave or pulsed lasers (1064 and 1450 nm) and exhibit all of the defining features of PA, including a clear excitation power threshold (20 kW/cm2), exceptionally long rise time at threshold (608 ms), and a dominant excited-state absorption that is >13000 times larger than ground-state absorption. Intriguingly, the nonlinearity of the ANPs emission (emission intensity versus pump power) can reach up to 26, remarkably higher than the maximum nonlinearities of order 7 in current lanthanide-based nanosystems. Such giant nonlinear optical response of the ANPs enables realization of photon-avalanche single-beam super-resolution imaging (PASSI) with sub-70 nm spatial resolution based on simple scanning confocal microscopy.
The claims made by the authors are justified, novel and exciting from both fundamental and applied point of view, especially in the fields of PA and super-resolution imaging. They are interesting not only for the community working on photon upconversion or super-resolution bioimaging, but also for a broad audience. The result presented in current work is striking and impactful as it represents a substantial advance in comparison with those previously reported and thus is a breakthrough in the development of PA materials and lanthanide nanoprobes for super-resolution bioimaging. I'm please to recommend the manuscript for publication in the top-impact journal Nature for its highest novelty and significance. Some minor concerns are noted below.

1. It would be very nice if the authors could provide a table to summarize the lanthanide-based PA and energy-looping upconversion materials (e.g., the size of the materials, working temperature, nonlinearity, and power threshold), which helps reader better understand the research background of lanthanide-based PA.
2. Why did the authors select NaYF4 as the host material for Tm3+ doping to achieve the giant PA upconversion? Can such giant nonlinearity (s = 26) of PA be realized in other lanthanide-doped NPs? What is the influence of the crystalline parameters, crystal-field strength, and local site symmetry of the host on PA of lanthanides? The authors are suggested to provide detail discussion about these aspects (in either the main text or Supplementary Materials), which are very important for future design and development of ANPs.
3. Fig. 1c: There is a mistake in the labeling of R2 in Fig. 1c. Please check it.
4. Lines 132-133: The authors stated that the rise time (608 ms) of the ANPs is nearly 400-fold the lifetime of the 3F4 state of Tm3+. However, the PL lifetime of Tm3+ 3F4 state is normally shorter than 100 μs due to the serious non-radiative relaxation process or cross-relaxation between the neighbouring Tm3+ ions. Please check it.
5. Fig. 3c: How did the authors calculate the QYs of ANPs? The details should be provided in the Supplementary Materials.
6. The authors are suggested to supplement a table which compares the PASSI with other existing super-resolution bioimaging techniques (e. g., super-resolution stimulated emission depletion

microscopy, nonlinear structured illumination microscopy, and near-infrared emission saturation nanoscopy) based on lanthanide nanoprobes or other luminescent materials. Comments on the advantages and limitations of these super-resolution bioimaging techniques are also helpful.
7. Some typos or grammar errors should be checked carefully. For example, line 219: (Fig. S9, 10;); Fig. S2: Tm3; page 9 of the Supplementary Materials: “3H5” should be “3H4”…

Xueyuan Chen

Referee #3 (Remarks to the Author):

The authors of the manuscript "Giant nonlinear optical responses from photon avalanching nanoparticles" describe their results on photon avalanche (PA) upconversion (UC) observed in Tm3+ doped NaYF4 nanoparticles and discuss potential applications of PA for super-resolution microscopy. The observed optical phenomena represent all features of PA including sharp threshold in optical pump intensity and critical slowdown of the fluorescence buildup at the threshold. Due to high non-linearity of the PA, the authors could demonstrate significantly improved spatial localization of individual nanoparticles.

While the results presented in the manuscript are of high quality and certainly worth publication. However, I doubt the sufficient novelty to qualify as breakthrough.

PAUC in rare-earth-based materials is known since 1979. It is based on efficient energy transfer between Ln3+ dopants closely packed in the host material once doped at sufficiently high concentration. Since this energy transfer depends on the very local, less than a nanometer, spacing between the dopants, there is no conceptual difference between PAUC in bulk and in nanosized material. If some real application of PAUC in nanoparticles was demonstrated, that would have changed the status of the work. However, the authors only demonstrate the phenomenon known for over 40 years though for nanosized material.

Apart from this major concern, I would like to mention that the manuscript contains some unsupported and sometimes even false statements. Let us start from the abstract. The authors write: "However, the photon avalanching (PA) mechanism underlying these optical innovations has been observed only in bulk materials and aggregates6,7 , and typically at cryogenic temperatures5-8". At the same time, they reference the work [5], in which there exists Table 2 showing that 45% of the PAUC materials investigated by the year 1999 exhibit PA at room temperature. The same claim is later repeated in the main text: " PA has been observed mostly at cryogenic temperatures5-8, with a few room-temperature exceptions6,7,22-25". 45% is not a few exceptions.

The authors write: "In conclusion, we report a new class of steeply nonlinear nanomaterials, realizing PA in engineered nanocrystals at room temperature with continuous wave pumping." They do not report a new class of materials, this is one material in terms of dopant-host combination.

The authors write: "these results immediately open new applications in ultrasensitive IR photon detection". I strongly doubt that PA would ever be able to compete with superconducting light detectors that can work up to 5-6um in wavelength, are more or less wavelength-independent, and have 90+% quantum efficiency.

The authors write: " More generally, by moving beyond the standard mechanisms, PA can not only enhance upconverting brightness and efficiency, but also offers unprecedented opportunities for technological innovation, since extremely nonlinear materials with controllable properties are essential for new electronic, photonic, and energy management technologies needed to address the growing societal demands for rapid and energy efficient sensing, information processing and

transduction." The mechanism is pretty standard and is described as a second order phase transition (see Ref.[26] of the manuscript). Furthermore, the statement sounds as if the PA was capabale of solving all technological problems without giving a single example of "unprecedented opportunities for technological innovation".

Coming to the second part of the manuscript, namely, super-resolution imaging with PAUC nanoparticles, I would like to raise several concerns. First of all, imaging nanoparticles dried on the glass slide and that of the same nanoparticles in a more complex environment are very much different. For immobilized nanoparticles it is easy to adjust the pump intensity very close to the PA threshold and, therefore, obtain high localization. Once they are in solution, the rotation of the nanoparticle will lead to turning of the Ln3+ ESA dipole with respect to pump polarization and, therefore, will make imaging close to PA threshold impossible. Second point: imaging of PAUC nanoparticles is intrinsically based on scanning the excitation beam through the emitting species, similar to confocal or STED microscopy. Thus, the image is supposed to be collected pixel-by-pixel with up to 600ms per pixel due to critical slowdown. Furthermore, the pixel size should be smaller than the expected resolution of the image, i.e. 65nm. Thus, in 1 second the authors would collect the fluorescence of two pixels, say, 30nm apart. In order to scan through the size of the focal spot of the excitation laser (300nm), 50 seconds are required. This is the minimal size of the area of a single beam in a multi-point approach. 50 seconds per frame differs drastically from the claimed rate of 1 frame/second. The third point: in order to obtain the localization accuracy of 2 nm, the authors have to work at the threshold and reduce their signal 10000 times (quote: "Finally, we note that in characterizing this PA system, we measure ~500-10,000-fold increases in emission intensity when pump intensity is increased from threshold to twice the threshold value").10000 times more signal means 100 time better SNR and, therefore, 100 better localization. Is PA really the better method to localise particles in light of these numerbers?

Author Rebuttals to Initial Comments:

Referees' comments:

Referee#1

Referee report on ‘Giant nonlinear optical response from photon avalanching nanoparticles’ by Changhwan Lee et al. The manuscript describes important and impressive results on the observation and application of photon avalanching (PA) in Tm3+ doped NaYF4 core-shell nanoparticles (NPs). The work is convincingly presented: the steep power dependence and the long onset times just above the pumping threshold are clear signatures of the PA phenomenon and beautifully demonstrate that the observed effect results from a true photon avalanche in the Tm-doped NPs. The work is expected to have a large impact. Various research areas where the extreme non-linearity can be used are mentioned and one (high resolution confocal imaging) is shown to work. The demonstration of a spatial resolution around 70 nm is impressive and indeed much simpler to achieve than with other methods that are presently used to beat the diffraction limit. Based on this assessment, I support publication of this work in Nature. There are some questions that should be addressed or clarified before publication. The various points I found appear mostly ‘chronologically’ (in the order the appear in the manuscript) or, where appropriate, by jumping to related sections in the Supplementary Materials. None of the issues are too serious as they do not affect the validity of the main results and conclusions of the manuscript.

Our reply: We thank the reviewer for their strong support, noting that our work “is expected to have a large impact”, that the sub-diffraction imaging application is “impressive and indeed much simpler to achieve than with other methods”, and that the “true photon avalanche” is “beautifully demonstrate[d]”. We appreciate the careful reading and have fully addressed the reviewer comments here and in the revised manuscript.

Reviewer comment: 1. Abstract – In the abstract it is mentioned that the avalanching NPs can be pumped with continuous wave or pulsed lasers. This initially confused me, as PA is a process observed for CW pumping (and cannot be excited with a laser pulse as it relies on building up population in the intermediate level during CW excitation). In the supporting information it became clear that some experiments (1450 nm excitation) were done with a pulsed 80 MHz femtosecond OPO laser. For the present experiments this is analogous to CW excitation as all effects take place on much longer timescales than the 12 ns intervals between the 200 fs pulses of the OPO. In their conclusions the authors seem to realize this and indicate 'realizing PA in engineered nanocrystals at room temperature with continuous wave pumping'. No mention of pulsed excitation there. I suggest to also leave 'pulsed lasers' out in the Abstract.

Our reply: We agree that here the pulsed excitation with a repetition rate of 80 MHz is analogous to continuous-wave excitation, and we have removed "pulsed lasers" from the Abstract.

Changes to the manuscript: The Abstract sentence now reads:

"Avalanching nanoparticles (ANPs) can be pumped by continuous-wave lasers and exhibit all of the defining features of PA."

Reviewer comment: 2. Figure 1 – The length of the arrows represents the energy of the photons and this is mostly correct. However, for the green arrows, representing the cross-relaxation process, one arrow is longer than the other as the 3H4-3F4 energy difference is larger than the 3H6-3F4 energy difference. This makes the cross-relaxation process phonon assisted. My suggestion is to adapt the length to make them the same and use the curvy light grey arrow to make clear that phonon emission is involved (similar to the way other phonon relaxation processes are shown in Figure 1). The need for phonon-assistance to make up for the ~1200 cm^{-1} energy mismatch is not really addressed in the manuscript - it is not unimportant as it may help in e.g. understanding differences in the dynamics in comparison with Tm3+ in other hosts with higher phonon frequencies (such as YAG).

Our reply: We agree that phonon assistance is important and would help clarify the PA mechanism. We have made the green arrows the same length and added a curvy grey line to the cross-relaxation process as shown in Fig 1c, and added specific mention of the ~1200 cm^{-1} energy mismatch in the manuscript.

Changes to the manuscript: We have updated Fig 1c to include phonon transitions:

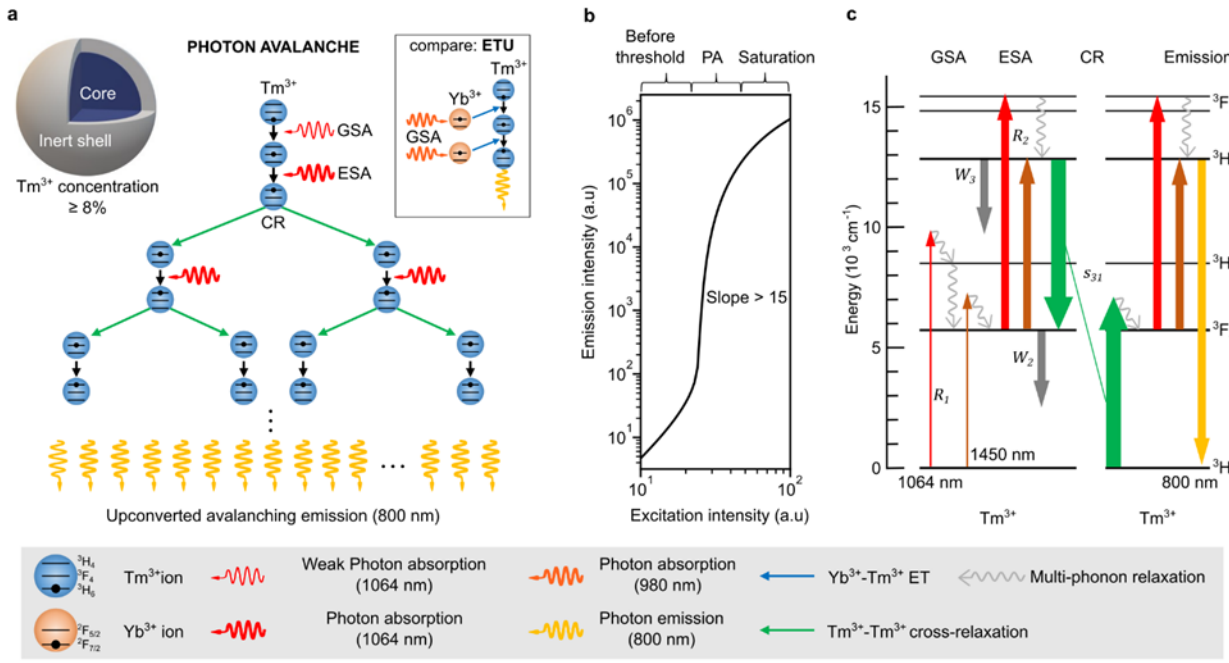

Fig. 1 Photon avalanching mechanism in Tm^{3+}-doped nanocrystals. a, Schematic of core/shell ANPs, with avalanching occurring when core Tm^{3+} concentration is ≥ 8%. (Inset) Standard ETU process, in which Yb^{3+} ions sensitize ground state absorption, precluding PA. **b,** Model plot of emission intensity vs. excitation intensity, showing the three stages of PA behavior. **c,** Energy levels of the $4f^{12}$ manifolds of Tm^{3+}. R1, R2 = ground- and excited-state excitation rates, respectively. W_2, W_3 are the aggregate rates of relaxation from the $^3F_4$ and $^3H_4$ levels, respectively. These rates account for radiative and nonradiative relaxation pathways but exclude cross-relaxation (CR) and other energy transfer processes. s_{31} = CR rate.

We have also clarified the text on page 2: "The cross-relaxation process is accompanied by the emission of phonons to compensate an energy mismatch of ca. 1200 cm^{-1}."

Reviewer comment: 3. Figure 1 – W_2 and W_3 are mentioned to be the $^3F_4$ and $^3H_4$ decay rates. Here, and elsewhere in the manuscript it would be good to be more specific and define already in the beginning what is meant with decay rate. For the 3F4 level W_2 is the sum of the radiative and non-radiative decay rates ($W_2^R + W_2^{NR}$). For the $^3H_4$ level the decay rates include radiative and non-radiative decay from the $^3H_4$ level as well as the strongly concentration dependent cross-relaxation rate s_{31} which is not included in W_3 but considered separately. It would be good if this could be more clearly outlined.

Our reply: We agree and have added definitions of W_2 and W_3 to the caption for Fig 1.

Changes to the manuscript: The Fig 1 caption now includes: "W_2, W_3 are the aggregate rates of relaxation from the $^3F_4$ and $^3H_4$ levels, respectively. These rates account for radiative and nonradiative relaxation pathways but exclude cross-relaxation (CR) and other energy transfer processes. s_{31} = CR rate"

Reviewer comment: 4. Figure 1 – small detail: include 'concentration' after Tm^{3+} in Tm^{3+} > 8%.

Our reply: Thank you for catching this, and we have added the word "concentration" after Tm^{3+}.

Changes to the manuscript: The Fig 1 caption now reads: "**a,** Schematic of core/shell ANPs, with avalanching occurring when core Tm^{3+} concentration is ≥ 8%."

Reviewer comment: 5. At several places the non-resonant GSA is mentioned. For people unfamiliar with lanthanide spectroscopy this may be puzzling as non-resonant excitation is not possible (apart from some fancy spectroscopy experiments driving transitions slightly off resonance, e.g. to observe changes in the Rabi frequency). In fact, the excitation here is resonant, but with a weakly absorbing vibronic overtone. I noticed that the excitation is chosen to be about 1500 cm-1 above the resonant level ($^3F_4$ for the 1450 nm excitation and $^3H_5$ for the 1064 nm excitation). I assume this was chosen deliberately to excite (resonantly) in the very weak 3rd or 4th vibrational overtone of the $^3H_4$-$^3F_4$ or $^3H_4$-$^3H_5$ electronic transitions. Vibronic coupling is extremely weak for lanthanides which makes the oscillator strengths of these 'non-resonant' excitations very small, indeed some 10^4 times weaker than excitation resonant with the purely electronic f-f transitions. It would be helpful to briefly explain the origin of the 'non-resonant' excitation and the background of the 10^4 ratio of ESA-to-GSA.

Our reply: We agree with the Referee's suggestion and point about GSA being a weak phonon-assisted transition in our system. We have changed "non-resonant" to "weak" in Fig. 1 and associated discussion. Further, we have included additional explanation regarding the phonon-assisted nature of the transition and its small oscillator strength in the PA mechanism discussion section of the Methods.

Changes to the manuscript: "non-resonant" has been changed to "weak" in Fig. 1. Also, an explanation of why GSA is very weak has been added in the Methods:

> "The ESA is effective because the absorption peak for the electronic $^3F_2$-$^3F_4$ transition is close to the 1064 nm excitation wavelength. However, the 1064 nm photons have an energy mismatch of ~1200 cm^{-1} for the electronic $^3H_6$-$^3H_5$ transition, which decreases the GSA cross section at that wavelength. Due to the energetic mismatch, GSA is a phonon-assisted process in this case, which makes its oscillator strength very small, ~10^4 times weaker than for excitation resonant with the purely electronic f-f transitions."

Reviewer comment: 6. Figure 2 concerns measurements of a thin film of drop casted NPs, providing an ensemble result. At other places in the manuscript and Supplementary Materials it is not always clear if it concerns single NP measurements or ensemble NP measurements. I assume Figs 2 and 3 in the main text and Figs S3, S4 all concern ensemble measurements on nanoparticle films. In Fig S7 this is clearly indicated. A short mention of this would be helpful. It could be interesting to study differences between individual (single) nanoparticles from the same batch which are expected to show different onset behavior depending on the variations of non-radiative processes in NPs with less/more defects, better/worse passivating shell.

Our reply: We are grateful for the careful reading and have clarified the manuscript on single vs. ensemble measurements. We strongly agree that studying the different characteristics of single nanoparticles and correlating with minor variations in shell thickness or other characteristics would be extremely interesting, as well as challenging (we are currently in the initial stages of designing an extensive correlated structure-function single-ANP study along these lines).

Changes to the manuscript: We have now noted in the Fig. 2, Fig. 3, and Figs. S3,5,8,9 captions that measurements were on ensemble films.

Reviewer comment: 7. The modelling is done using a model developed by Guy and Joubert for microcrystalline materials. Qualitatively, the results are consistent and the trends observed upon decreasing the W2NR rates by growing thicker shells and/or making bigger cores are in line with the expectations, shifting the threshold for PA to lower powers with decreasing W^2_{NR}. Quantitatively, the modelling is not clearly explained and assumptions are made that seem not correct. The Supporting

Materials do not really help. It would be helpful to describe the procedure more clearly and be consistent.

Our reply: We appreciate the importance of clarifying the differential rate equation model, as well as offering justification for the parameters and fittings. We have modified the supplementary section explaining our rate equation model to make it clearer and more specific. The terms in the differential rate equations are now unified with those in the main text, and the Judd-Ofelt parameters are given in addition to the relaxation rates.

Changes to the manuscript: See below, for point-by point changes.

For example:

Reviewer comment: s_{31} in the Main Text seems to be s_3 in Supp. Mat.

Our reply: The reviewer is correct and we have updated the nomenclature.

Changes to the manuscript: Terms in the equations in Supplementary materials have been unified with those in the manuscript.

Reviewer comment: The branching ratio b_{32} is (I assume, it is not explained) the radiative decay from $^3H_4$ to $^3F_4$, feeding the $^3F_4$ level. The role of the $^3H_5$ level is not clear. From the $^3H_5$ level, there will be fast relaxation to the $^3F_4$, also feeding 'level 2'. Is radiative decay from $^3H_4$ to $^3H_5$ included in b_{23}?

Our reply: We thank the referee for catching this; we agree that a definition of the term is needed and apologize for missing it previously.

Changes to the manuscript: We now define the variable b_{32} in the modeling discussion of the SI:

"These equations involve the ground-state and excited-state absorption coefficients σ^{GSA} and σ^{ESA}, radiative and non-radiative relaxation rates W_i^R and W_i^{NR} (excluding cross-relaxation) of level i, the branching ratio b_{32} (the sum of radiative relaxation rates from the $^3H_4$ level to intermediate levels divided by W_3^R), and the cross-relaxation rate s_{31}."

Reviewer comment: Table S3 has as a header 'Judd-Ofelt parameters and reduced matrix elements. It would be wonderful to include these parameters (Judd-Ofelt parameters Ω2, Ω4 and Ω6 and reduced matrix elements U(2), U(4) and U(6) for all relevant transitions) since then we could calculate the branching ratio b23, the absorption cross section σESA, W2R, W3R etc. However, the table does not contain these parameters, but rather contains some numbers that seem to have been calculated from these parameters that were taken from data on $Na_{0.4}Y_{0.6}F_{2.2}$:Tm^{3+} crystals. In a revised version it would be helpful to provide the Judd-Ofelt parameters and reduced matrix elements used, as well as a justification that the numbers for $Na_{0.4}Y_{0.6}F_{2.2}$:Tm^{3+} are also valid for β-$NaYF_4$:Tm^{3+}. Did the authors check if σ_{ESA} calculated with these Judd-Ofelt parameters matches the $5.6x10^{-25}$ m^2 found here for the $^3F_4$-$^3H_4$ transition?

Our reply: This is a good point; we had used the Judd-Ofelt parameters from $Na_{0.4}Y_{0.6}F_{2.2}$:Tm^{3+} following our previous modeling work, which were the closest values we had at the time. We agree that there are differences between that structure and β-$NaYF_4$: Tm^{3+}, and that the usage of the parameters for the calculation of radiative relaxation rates of β-$NaYF_4$: Tm^{3+} cannot be confidently justified at a fully quantitative level because those two stoichiometries have different crystal structure and phonon energies: Tm^{3+} in $Na_{0.4}Y_{0.6}F_{2.2}$ and β-$NaYF_4$ are 8- and 9-fold coordinated, respectively. We have now found and implemented Judd-Ofelt parameters for β-$NaGdF_4$:Tm^{3+} crystals reported in Villanueva-Delgado *et al*, Journal of Luminescence 189 (2017) (This paper is also now cited in our Supplemental

materials). It has equivalent crystal structure to $NaYF_4$ and a comparable phonon energy. All modeling and fitting results in our paper now utilize these updated parameters.

We also agree that the comparison of σ_{ESA} values calculated from rate equation simulation and Judd-Ofelt theory is helpful. We have now estimated the σ_{ESA} value at 1064 nm using Judd-Ofelt parameters following our previous approach (this approach is now outlined in the SI, following Chem. Soc. Rev. 44, 1653 (2015)), which gives a value of the same order (~3 X 10^{-25} m^2 compared to the 6.4 X 10^{-25} m^2 obtained from our model's fit to the experimental data), values that are consistent within the known uncertainties of the approach given the assumptions inherent in the calculation method. Also, we have added a table for the comparison of σ_{ESA} from our simulation and an experiment with Tm-doped silica fiber (the closest ESA spectrum we could find). Using phonon energies of two host materials, which influence the shape of the absorption spectrum, we can additionally indirectly check the validity of the obtained σ_{ESA} values.

Changes to the manuscript: All curves and values from the rate equation simulations have been updated in the manuscript and SI using the Judd-Ofelt parameters for β-$NaGdF_4$:Tm^{3+} crystals (and a reference has been added), including the model fits to the experimental data in Figs. 2 and 3 (see below). Judd-Ofelt parameters and reduced matrix elements have been added to the SI (Tables S4,5; see below). Also, a table for the comparison of σ_{ESA} from our rate equation simulation fits to our data and experiment with Tm-dope silica fibers has been added to the SI; Table S8 (also below). Finally, we have added a statement in the SI on the ESA cross-section calculation from J-O parameters (copied below), as well as a reference to Chem. Soc. Rev. 44, 1653 (2015).

"Absorption cross sections ($\sigma_{int,ESA}$), integrated over the entire ESA peak, are calculated from Judd-Ofelt theory using the methods described in a recent review[13]. The ESA cross section $\sigma_{ESA}(\bar{\nu})$ at a given excitation wavenumber ($\bar{\nu}$) is calculated by assuming that the ESA absorption peak has a Gaussian lineshape with variance w^2 (w = FWHM/($2\sqrt{\ln(2)}$)."

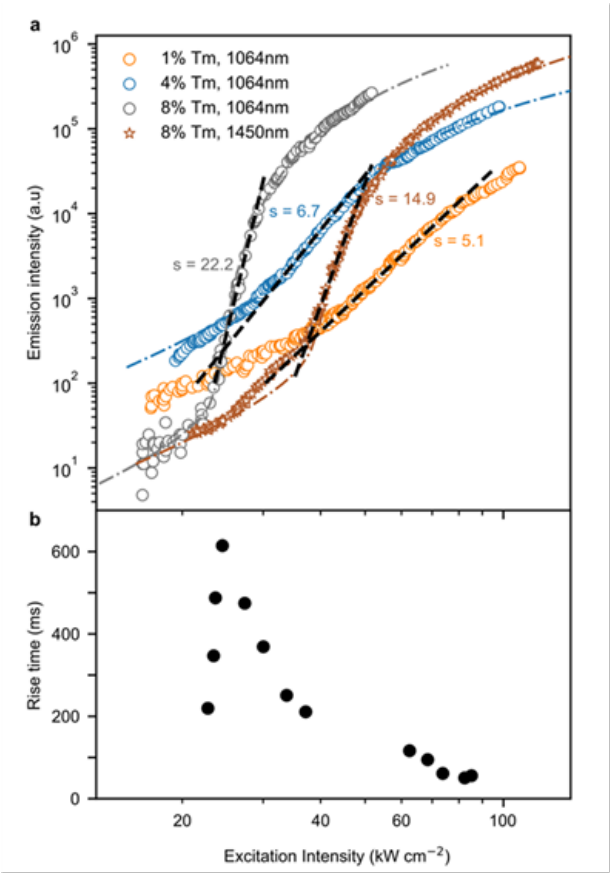

Fig. 2. Demonstration of nanoparticle photon avalanching. a, 800 nm emission intensity vs. excitation intensity for ensemble films of 1%, 4%, and 8% Tm^{3+}-doped nanocrystals. 1064 nm excitation is used, except where noted. See Tables S1,2 for ANP sizes. Photon avalanching is also achieved in the 8% Tm^{3+} ANPs with 1450 nm excitation (brown stars). The dash-dotted lines are fits of the PA DRE model to the data, as described in the text and SI. **b**, 800 nm emission rise times vs. excitation intensity for 8% Tm^{3+} ANPs in (a), showing a large increase, up to 608 ms, near the PA threshold.

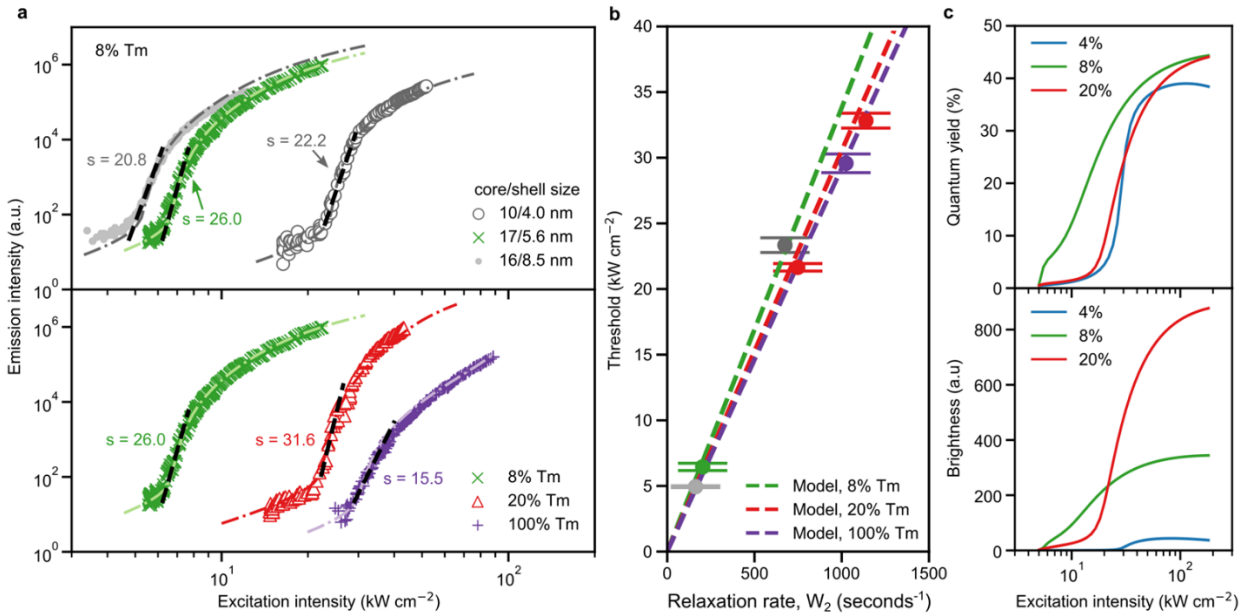

Fig. 3. Modifying PA kinetics via ANP shell thickness, surface-to-volume ratio, and Tm^{3+} content. a, top panel. 800 nm emission intensity vs. 1064 nm excitation intensity curves for different core sizes/shell thicknesses of 8% Tm^{3+}-doped ANPs. bottom panel: ANPs with different Tm^{3+} concentrations. Green × symbols: 8% Tm^{3+}, same as top panel. Red triangles: 20% Tm^{3+}, (see SI for sample details; sample 7 data shown; curve for sample 6 with 20% Tm^{3+} is shown in Figs. S3,5). Purple + symbols: 100% Tm^{3+}. See SI Tables S1,2 for measured dimensions and their standard deviations. The dash-dotted lines are fits of the PA DRE model to the data. All measurements on ensemble films. **b,** Plot of threshold intensity vs. W_2 extracted from the data in (a), showing linear dependencies on W_2, with slopes that depend on s_{31}. Error bars are determined from the standard deviations of the curve fittings shown in Fig. S3. **c,** calculations of upconverting quantum yield and d, brightness vs. excitation intensity for 4%, 8%, and 20% Tm^{3+}, using values from model fits to the green circles and red squares in (a), and the blue circles in Fig. 2a.

Table S4. Judd-Ofelt and relaxation parameters

Parameter	***Value***
Ω_2 (10^{-20} cm^2)	2.37
Ω_4	3.05
Ω_6	0.41
W_2^R (s^{-1})	162.60
W_3^R (s^{-1})	636.01
b_{32}	0.144

Table S5. Reduced matrix elements for Tm^{3+} ion[4]

Electronic Transition	$[U^{(2)}]^2$	$[U^{(4)}]^2$	$[U^{(6)}]^2$
$^3H_6 \rightarrow {}^3F_4$	0.5395	0.7261	0.2421
$\rightarrow {}^3H_5$	0.1074	0.2314	0.6385
$\rightarrow {}^3H_4$	0.2357	0.1081	0.5916
$^3F_4 \rightarrow {}^3H_5$	0.0909	0.1299	0.9264
$\rightarrow {}^3H_4$	0.1275	0.1311	0.2113
$^3H_5 \rightarrow {}^3H_4$	0.0131	0.4762	0.0095

Table S8. Phonon energy of host lattice and absorption cross section at 1064 nm

Host lattice	*Phonon energy* (cm^{-1})	**Absorption cross section at 1064 nm, σ^{ESA}** ($\times 10^{-25}$ m^2)
$\beta - NaYF_4$	~360	6.4 (DRE model fit to data)
Silica fiber	*~1050*	*3.5* (from experiment)

Reviewer comment: $W^3{}_{NR}$ is taken as a constant and is (it seems) determined from the non-radiative multi-phonon relaxation rate in the microcrystalline $Na_{0.4}Y_{0.6}F_{2.2}$:Tm^{3+} material. $W_2{}^{NR}$ is not taken from this reference but fitted from the curves and found to vary and increase when non-radiative channels become more prominent in samples with smaller nanocrystal cores, thinner shells or higher doping concentrations. This variation is consistent with what is expected and indeed this changes the threshold for the PA effect in a logical manner. However, keeping $W_3{}^{NR}$ constant seems not logical. Would the same variation in non-radiative decay found for $W^2{}_{NR}$ due to surface defects and phonon assistance not also be true for $W^3{}_{NR}$? The energy gaps for non-radiative decay $W^2{}_{NR}$ ($^3F_4$-$^3H_6$, ~5000 cm^{-1}) and $W_3{}^{NR}$ ($^3H_4$-$^3H_5$, also ~5000 cm^{-1}) are similar. At least, it should be mentioned why $W_2{}^{NR}$ is assumed to vary while $W_3{}^{NR}$ is taken as constant with a short explanation why this is allowed.

Our reply: This is an excellent suggestion by the referee. Previously, we kept $W_3{}^{NR}$ constant during the fitting procedure even though the $^3H_4$-$^3H_5$ transition, a main relaxation path for $W_3{}^{NR}$, has a similar energy gap to that of the $^3F_4$-$^3H_6$ transition. Now we have modified our rate equation model by both using new Judd-Ofelt parameters (as described above) and setting $W_3{}^{NR}$ as an independent variable. As a result, Figs. 2 and 3 and several numbers from the simulation in the manuscript are updated accordingly. Now, with these updated inputs, the ESA-to-GSA ratio has changed from 13,000 to 10,667, still above 10,000, a criterion for achieving a clear photon avalanche threshold.

Changes to the manuscript: The newly derived nonradiative rate numbers have been added to the SI Table S7 and the updated ESA-to-GSA ratio has been included in the main text and added in SI Table S6 (see below).

Table S7. Derived phonon-assisted non-radiative relaxation rates from curve-fitting

Parameter	***Sample No.***						
	2	***3***	***4***	***5***	***6***	***7***	***8***
W_2^{NR} (s^{-1})	56.9	512	40.7	~0	976	585	862
W_3^{NR} (s^{-1})	103.58	1030	87.3	~0	1957	1176	1730

Table S6. Derived absorption coefficients and coefficients for energy transfer between ions from curve-fitting

Parameter	***value***	
σ^{GSA} ($\times 10^{-25}\ m^2$)	6.0×10^{-4}	
σ^{ESA} ($\times 10^{-25}\ m^2$)	6.4	
a_{cr} (s^{-1})	160	c > 4%
	49.7	c = 4%
a_{inv} (s^{-1})	25.6	c > 4%
	6.67	c = 4%
a_{uc} (s^{-1})	9.00	c > 4%
	2.35	c = 4%

Reviewer comment: It would have been good if changes in the changes in W_2 that were extracted from the data in Fig. 3(a) were independently verified by luminescence decay measurements of the 3F4 emission under pulsed excitation.

Our reply:

We also agree that it would be good to measure luminescence decay lifetime at the $^3F_4$ manifolds, but unfortunately our experimental setup is not yet equipped with an IR detector required for this wavelength range (our system currently uses Si detectors). We would like to do this in a follow-up/future study. Instead, we measured the time-resolved luminescence from the $^3H_4$ level and compared with the time-resolved luminescence modeling from DRE simulation. The experimental data agrees nicely with the simulation result, as shown below. We note that the data from simulation and experiment show shorter lifetime at low excitation intensity because the rate of cross relaxation is proportional to the population at the ground state which decreases with increasing excitation intensity.

Changes to the manuscript: A comparison DRE simulations and experimental measurements of time-resolved luminescence from the $^3H_4$ - $^3H_6$ transition have been added to the SI (Fig. S8)

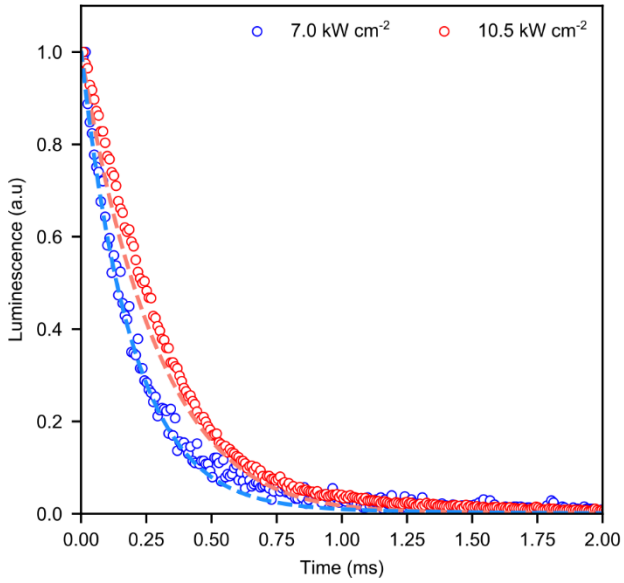

Fig. S8. Comparison of time-resolved luminescence of the $^3H_4$ -$^3H_6$ transition (800 nm) of $NaYF_4$:8% Tm^{3+} nanocrystal ensembles from DRE simulations and time-resolved luminescence measurements on ensembles. Blue: excitation intensity = 7.0 kW cm^{-2}; Red: excitation intensity = 10.5 kW cm^{-2}. Dashed lines are from the DRE simulations; symbols are experimental data.

Reviewer comment: 8. The paper sometimes requires more effort than necessary to understand. In the main text sample variation is discussed for three different types of 8% Tm3+ samples. The results are in line with what is expected (thicker shell/larger particles results in a lower PA threshold because of less non-radiative losses W_2^{NR}). However, in Figure 3b there also seems to be a second type of 20% sample. This is used to determine the slope differences in that depend on s31. Besides my feeling that these slope differences in Fig. 3b are not really convincing, I wondered what the second 20% sample was. I could not find it in the main text. The Supp. Mat. shows indeed two different 20% NPs: Sample 6 and Sample 7 with a 17.5 nm core (sample no. 6) and a 10.4 nm core (sample no. 7) with the same 2.6/2.7 nm shell thickness. In Figure S3 it is shown that they have a different onset of the PA effect (note the x-axis in Figure S3 is not given in kW cm-2 as in all other power dependence Figures but in W/cm2). It is however not indicated which curve belongs to sample 6 and which to sample 7. Table S5 may provide the answer: in Table S5 the 'phonon assisted non-radiative relaxation rates' W2NR are given for Particle No. 2 to 8 (maybe change Particle No. to Sample No?). Surprisingly, W2NR is lower for the smaller core sample 7 (513 s^{-1}) than for the larger core particle sample 6 (878 s^{-1}). Is the lower PA threshold in Figure S3 for the smaller particle 7? This would be consistent with the lower W_2^{NR} but unexpected as smaller core NPs are expected to have higher non-radiative decay (as observed for the 8% NPs). It is unfortunate that discussion on the two 20% samples is missing, especially since the trend seems opposite to what is expected and what was observed for the 8% samples. In Table S6 the second 20% sample is missing again. It would be nice to see and compare the Δ_{av} values for the two 20% Tm3+ samples with different core sizes.

Our reply: We thank the Referee for pointing out the inconsistency of the relationship between the core sizes and multiphonon relaxation rates of samples 6 and 7 in the Supplementary material. We realize we made an error in Table S1: while Fig. S1 is labeled correctly, we had switched the sizes for samples 6 and 7 in Table S1. The two different sizes indeed follow the expected trend, with the larger core showing a lower threshold intensity (and lower W_2).

To better highlight that we studied two different sizes of 20% ANPs, we have now added explicit mention of the two samples both in the main text description of Fig. 3, as well as in the Fig. 3 caption. Additionally, we have added the Δ_{av} figure of merit value for both 20% Tm ANP samples to Table S9, and regret overlooking its inclusion in the original submission. Finally, new SI Fig. S5 has been added, which compares within a single plot the pump intensity vs. emission intensity curves for all samples studied.

Changes to the manuscript: We have now added explicit mention of the two 20% Tm ANP sizes to the manuscript:

"To study this effect, core/shell ANPs with 20% and 100% Tm^{3+} were synthesized (including 2 sizes of 20% Tm^{3+} particles; SI), and threshold intensity is found to increase with increasing Tm^{3+} content (Fig. 3a, bottom panel)."

And to the Fig. 3 caption:

"Red triangles: 20% Tm^{3+}, (see SI for sample details; sample 7 data shown; curve for sample 6 with 20% Tm^{3+} is shown in Figs. S3 and S5)."

The sample size information has also been corrected and updated in Table S1:

Table S1. The average core diameters and shell thicknesses of $NaYF_4$: 1-100% Tm^{3+}@ $NaY_{0.8}Gd_{0.2}F_4$ core-shell nanocrystals

Sample No.	Tm concentration	Core diameter	Shell thickness
1	1%	15.8 ± 1.5 nm	3.0 ± 1.2 nm
2	4%	14.1 ± 1.5 nm	3.8 ± 1.0 nm
3	8%	10.2 ± 1.1 nm	4.0 ± 0.8 nm
4	8%	17.3 ± 0.8 nm	5.6 ± 0.9 nm
5	8%	15.9 ± 1.0 nm	8.5 ± 1.9 nm
6	20%	10.4 ± 1.0 nm	2.7 ± 0.9 nm
7	20%	17.4 ± 0.8 nm	2.6 ± 0.6 nm
8	100%	15.8 ± 1.3 nm	4.2 ± 1.0 nm

The Δ_{av} values for both 20% Tm ANP sizes are now included in Table S9:

Table S9. Increase in emission Δ_{av} when pump intensity is increased from the avalanche threshold pump intensity I_P^{th} to twice the threshold pump intensity $2I_P^{th}$.

	Sample No.	***Nanoparticle composition***	$\Delta_{av} = I_E(2I_P^{th})/I_E(I_P^{th})$, ***experiment (800 nm emission)***
Figure 2a	1	1% Tm (1064 nm)	26
	2	4% Tm (1064 nm)	34
	3	8% Tm (1064 nm)	2029
	3	8% Tm (1450 nm)	1025
	3	8%, core/shell = 10/4.0 nm	2029

Figure 3a upper panel	4	8%, core/shell = 17/5.6 nm	1347
	5	8%, core/shell = 16/8.5 nm	1190
Figure 3a bottom panel	3	8% Tm	1347
	7	20% Tm	9691
	8	100% Tm	491
An additional sample	6	20% Tm	6142

Finally, we have added new Fig. S5, which directly compares the pump intensity vs. emission intensity curves for all studied samples:

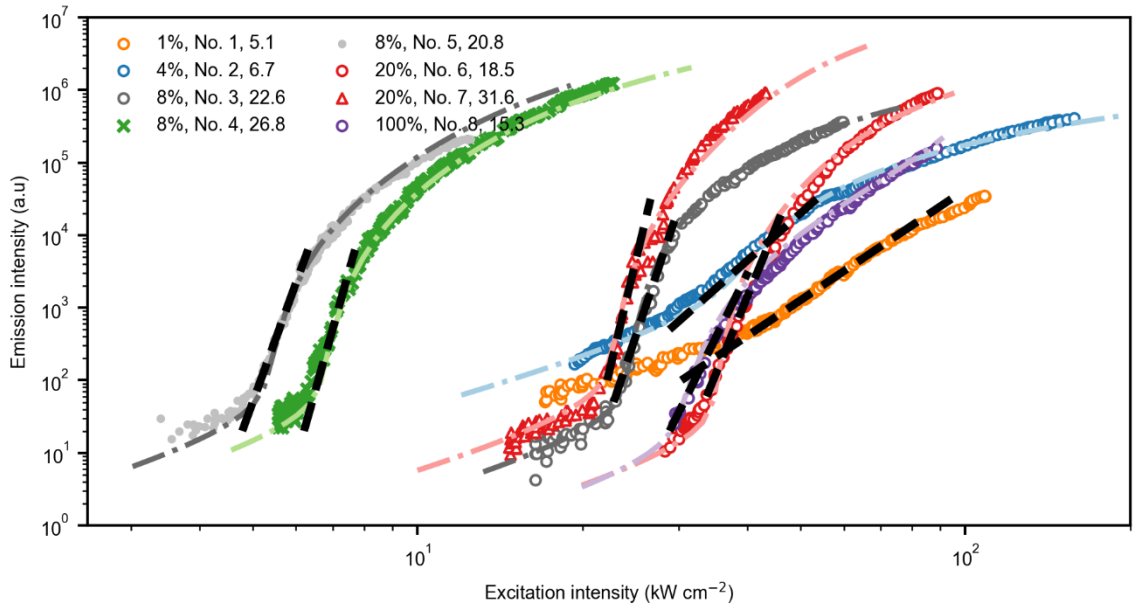

Fig. S5. 800 nm emission intensity vs. 1064 nm excitation intensity curves for different core sizes/shell thicknesses of 1-100 % Tm^{3+}-doped ANP ensembles. Tm^{3+} concentrations, sample numbers (see Fig. S1, Table S1), and slope values of the log-log curves are shown in the legend.

Reviewer comment: 9. Table S5 shows that W_2^{NR} rate for sample 5 is 0. This seems to be very low. It deserves some discussion. The very thick shell of sample 5 may completely suppress quenching.

Our reply: We found this interesting as well. Our modeling and fits indeed lead us to the same conclusion as the Referee: that the very thick shell of sample 5 effectively suppresses surface quenching. This is consistent with findings by Fischer, *et al.*, (Nano Lett. 16, 7241 (2016)), where shells > 6nm in thickness can prevent surface quenching. We also agree that this deserves more discussion, which has now been added in the SI regarding the low W_2^{NR} and W_3^{NR} for sample No. 5, as shown below.

Changes to the manuscript: Discussion on why W_2^{NR} and W_3^{NR} for sample No. 5 are assumed to be negligible are now added in the Supplementary Material.

"This model assumed W_2^{NR} and W_3^{NR} are negligible for sample no. 5 because multiphonon relaxation rates of Ln^{3+} ions in LaF_3 at the $^3H_4$ and $^3F^4$ levels, which has a comparable phonon energy to that of β-$NaYF_4$ [7,8], are calculated to be at least 4 order of magnitude smaller than other parameters. Also, the shell thickness is over 6 nm, which was reported to be thick enough to prevent surface quenching [9]."

Reviewer comment: 10. In Table S2 the core sizes for the elliptical particles are given for four samples which are the same as in Table S1 but now the numbers are given for the two axes which are used to determine the average diameter. For sample 1 this makes sense: (major axis + minor axis)/2 = (17.3+14.3)/2 = 15.8 nm – indeed the number in the column average and in Table S1. For sample 4, there is a 0.1 nm deviation – not a real problem. However, the number for the average (15.9 nm) is not the same as the number for sample 4 in Table S1 (17.3 nm). The numbers in Table S2 for samples 5 and 6 do not make sense at all, the minor axes are 4.0 and 3.0 nm – much too small, the average diameter for sample 6 (17.5 nm) is larger than that of the major axis (15.8 nm). Something seems to have gone wrong in Table S3– or I am missing something?

Reply: We thank the Referee for bringing attention to these notable typos in our Supplementary material. We had made errors when pasting in the values. We have corrected these tables, as shown below.

Changes to the manuscript: The correct values have been inserted into Table S2:

Table S2. The core sizes of nanoparticle samples with elliptical shapes

Sample No.	Tm concentration	Core diameter		
		Major axis	Minor axis	Average
1	1%	17.3 ± 1.1 nm	14.3 ± 1.3 nm	15.8 ± 1.5 nm
4	8%	19.8 ± 0.8 nm	15.1 ± 1.0 nm	17.3 ± 0.8 nm
5	8%	17.5 ± 1.4 nm	14.1 ± 1.3 nm	15.9 ± 1.0 nm
7	20%	19.5 ± 1.0 nm	15.5 ± 0.8 nm	17.4 ± 0.8 nm

Reviewer comment: 11. In line 178 it is mentioned that the quantum yield (QY) can exceed 20% for a pump power exceeding 10^5 W/cm2. In Figure 3c the QY is seen to exceed 40% and come very close to the theoretical maximum of 50%. Is the quantum yield defined as (number of 800 nm photons emitted)/(number of 1064 nm photons absorbed)? It will be good to mention 40% (and not 20%) if Figure 3c is correct and to clearly define quantum yield.

Our reply: The referee is correct: we indeed defined quantum yield as photons emitted divided 1064 nm photons absorbed. We have now added a more explicit definition to the SI (copied below). Also, Figure 3c is correct for our model when we assume very thick shells (no surface quenching, as in sample 5). We have now updated the main text to reflect the 40% value.

Changes to the manuscript: The main text has been revised to better reflect the 40% QY calculated value:

"Our calculations reveal that for fully passivated core-shell nanoparticles, QY can reach ~40% for ANPs excited beyond threshold at 10^5 W/cm^2 (Fig. 3c)."

We have added our definition and an equation for QY to the SI:

"Theoretical quantum yield (QY) for the $^3H_4 \rightarrow {}^3H_6$ transition (800 nm) can be calculated by using the results from the DRE simulation. The equation is expressed as:

$$QY = \frac{\#\ photons\ emitted}{\#\ photons\ absorbed} = \frac{(1-b_{32})W_3^R n_3}{\sigma^{GSA}\frac{I_p}{h\upsilon}n_1 + \sigma^{ESA}\frac{I_p}{h\upsilon}n_2}$$ "

Reviewer comment: I realize the number of comments is somewhat high considering the excellent quality of the work and my positive recommendation for publication. It is however good for important results as presented here to explain all aspects clearly and help readers to easily understand figures without having to put in too much effort. Also, it is important to make it possible to understand and reproduce the fitting/analyses by providing more details, such as the values used for the Judd-Ofelt parameters and reduced matrix elements in the Supp. Mat. My comments do not distract from the importance of a convincing demonstration of the strongly non-linear optical response in Tm3+-doped NPs. The origin is clearly identified as a photon avalanche effect and this is a breakthrough in the field. The potential impact is illustrated with confocal imaging experiments showing how the PA effect can serve to easily obtain spatial resolutions well below the diffraction limit. In the future the extreme non-linearity in these and other NPs showing photon avalanche effects may be used for other applications. As noted in the introductory paragraph, I therefore recommend publication in Nature and hope my remarks will be considered as helpful.

Our reply: The reviewer's detailed comments have helped us immensely to clarify our manuscript.

Referee #2 (Remarks to the Author):

In this manuscript, Schuck and co-workers reported a novel photon avalanching (PA) upconversion phenomenon at room temperature in heavily Tm3+ (>8 mol%) doped β-NaYF4 core/shell nanoparticles (NPs). The avalanching NPs (ANPs) can be pumped by either continuous-wave or pulsed lasers (1064 and 1450 nm) and exhibit all of the defining features of PA, including a clear excitation power threshold (20 kW/cm2), exceptionally long rise time at threshold (608 ms), and a dominant excited-state absorption that is >13000 times larger than ground-state absorption. Intriguingly, the nonlinearity of the ANPs emission (emission intensity versus pump power) can reach up to 26, remarkably higher than the maximum nonlinearities of order 7 in current lanthanide-based nanosystems. Such giant nonlinear optical response of the ANPs enables realization of photon-avalanche single-beam super-resolution imaging (PASSI) with sub-70 nm spatial resolution based on simple scanning confocal microscopy. The claims made by the authors are justified, novel and exciting from both fundamental and applied point of view, especially in the fields of PA and super-resolution imaging. They are interesting not only for the community working on photon upconversion or super-resolution bioimaging, but also for a broad audience. The result presented in current work is striking and impactful as it represents a substantial advance in comparison with those previously reported and thus is a breakthrough in the development of PA materials and lanthanide nanoprobes for super-resolution bioimaging. I'm please to recommend the manuscript for publication in the top-impact journal Nature for its highest novelty and significance. Some minor concerns are noted below.

Our reply: We are grateful to Professor Chen for his review and praise of our work as "striking and impactful as it represents a substantial advance", and "novel and exciting from both fundamental and applied point of view".

Reviewer comment: 1. It would be very nice if the authors could provide a table to summarize the lanthanide-based PA and energy-looping upconversion materials (e.g., the size of the materials,

working temperature, nonlinearity, and power threshold), which helps reader better understand the research background of lanthanide-based PA.

Our reply: This is a good suggestion and we have added the table summarizing previous representative reports of energy-looping in Ln-based nanomaterials to the supplementary information.

Changes to the manuscript: New comparison Table S10 has been added to the SI.

Reviewer comment: 2. Why did the authors select NaYF4 as the host material for Tm3+ doping to achieve the giant PA upconversion?

Our reply: We selected β-$NaYF_4$ as the host material because it has been shown previously to host efficient upconversion in both bulk and nanoscale materials. This material is probably the most common upconverting nanoparticle host in part due to its low phonon energy and the fact that it can readily incorporate lanthanide ions, even at high lanthanide concentrations. Also, syntheses of nanoparticles of this phase are well established, allowing other researchers to quickly reproduce our results. Notably, the surface of β-$NaYF_4$ can be passivated with undoped shells with high a degree of control (see e.g. JACS 139, 3275 (2017); Nano Lett. 16, 7241 (2016)). Such passivation is a routine step for enhancing the efficiency of lanthanide-doped β-$NaYF_4$ nanocrystals and is a prerequisite for functionalizing the nanoparticles with biomolecules. Such biofunctionalization protocols for $NaYF_4$ have been well established for a wide range of applications (see e.g. *Nat. Nanotechnol.* **10**, 924-936 (2015)). While alternative colloidal nanocrystalline host materials have been developed (e.g., CaF_2, $LiYF_2$, YAG, Y_2O_3, and phosphates), $NaYF_4$ hosts the most efficient upconversion luminescence and is one of the most straightforward and reproducible host materials to synthesize in the form of stable colloidal nanoparticles.

Reviewer comment: Can such giant nonlinearity (s = 26) of PA be realized in other lanthanide-doped NPs? What is the influence of the crystalline parameters, crystal-field strength, and local site symmetry of the host on PA of lanthanides? The authors are suggested to provide detail discussion about these aspects (in either the main text or Supplementary Materials), which are very important for future design and development of ANPs.

We agree that it is an interesting and relevant question whether such highly nonlinear behavior can be realized in other lanthanide-doped materials. The fact that other (larger) materials have exhibited photon avalanche suggests that there are opportunities to develop an entire class of PA probes for imaging and sensing, and this should be possible with other dopants (Pr^{3+}, Ho^{3+}, Er^{3+} also possibly co-doped with Yb^{3+}) and other crystalline host materials (e.g. (Li/K)(Y/Gd/Lu)F_4, (La/Ce)(Cl/B)$_3$, CdF_2, Y_2O_3, YAG, $YAlO_3$, $LnVO_4$) or even heavy glasses (e.g. ZBLAN) [M.F..Joubert, Opt. Materials 11 (1999)]. Therefore, the path we have demarcated for PA in nanoparticles (i.e. using PA preconditioning, lack of sensitizer, and surface passivation) may enable the design of a whole variety of PA wavelengths and their further biomedical and technological applications.

In general, the same factors that promote photon avalanche will encourage high nonlinearities, e.g., a high ESA/GSA ratio, high cross-relaxation and energy transfer rates relative to other relaxation pathways, as well as emission branching ratios. Crystal-field strength and local site symmetry will define the Stark splitting and number of Stark components, their oscillator strength and energy gaps, which ultimately will affect the ESA to GSA ratio or thermal equilibrium between some levels and Stark components. The number of possible sites to be substituted by lanthanide dopants will also contribute to ESA bandwidth and absorption cross section. The phonon energy and density of states, and thus crystalline structure of the host also plays a role in the efficiency of the phonon-assisted GSA and CR. Reducing the phonon energy of a host will proportionally increase the number of phonons required to bridge energy gaps between excitation radiation and GSA transition energies, and, according to the Energy Gap Law, exponentially decrease GSA transition rates.

The theoretical approached used in this work and our previous work (ACS Nano 10, 8423 (2016); Nanoscale Horizons 4, 881 (2019)) may provide a method to design a library of lanthanide-doped photon avalanche nanoparticles. As we describe in the manuscript, the CR rate s_{31} and relaxation rate W_2 may be fine-tuned by varying the Ln^{3+} concentration and by surface passivation, respectively. For larger variations in composition, we recognize that many material parameters are interdependent, which can complicate predictions of the optimal materials for PA. Crystal structure determines both site symmetry and phonon energies. Meanwhile changing dopant type results in different transition energies, cross-relaxation rates, and relaxation rates. Thus, in the future, high-throughput rate equation simulations that account for the above factors will be essential for rapidly screening the many combinations of material parameters for PA behavior.

Changes to the manuscript: Based on the reviewer's suggestion, a section titled "Considerations for future ANP designs" has been added to the SI, which includes the discussion provided above.

Reviewer comment: 3. Fig. 1c: There is a mistake in the labeling of R_2 in Fig. 1c. Please check it.

Our reply: We thank Prof. Chen for catching the error. We have edited Fig. 1c so that R_2 now labels the correct transition (ESA).

Changes to the manuscript: Fig. 1 has now been updated to reflect the proper R_2 transition (see below).

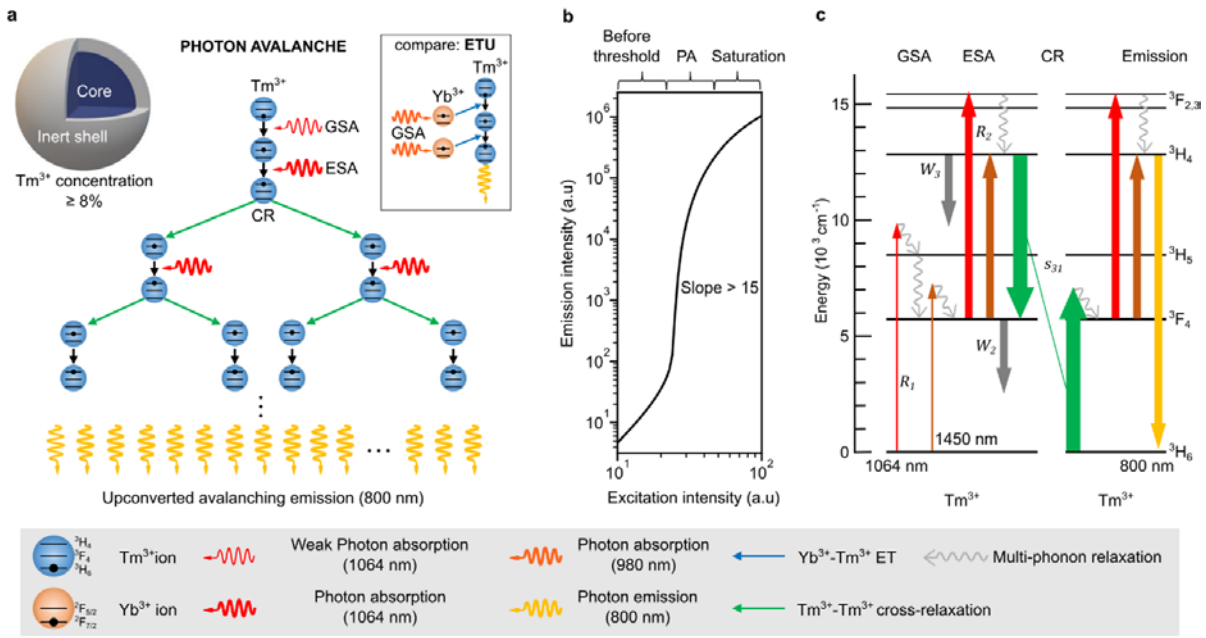

Fig. 1. Photon avalanching mechanism in Tm^{3+}-doped nanocrystals. a, Schematic of core/shell ANPs, with avalanching occurring when core Tm^{3+} concentration is ≥ 8%. (Inset) Standard ETU process, in which Yb^{3+} ions sensitize ground state absorption, precluding PA. **b,** Model plot of emission intensity vs. excitation intensity, showing the three stages of PA behavior. **c,** Energy levels of the $4f^{12}$ manifolds of Tm^{3+}. R_1, R_2 = ground- and excited-state excitation rates, respectively. W_2, W_3 are the aggregate rates of relaxation from the $^3F_4$ and $^3H_4$ levels, respectively. These rates account for radiative

and nonradiative relaxation pathways but exclude cross-relaxation (CR) and other energy transfer processes. s_{31} = CR rate.

Reviewer comment: 4. Lines 132-133: The authors stated that the rise time (608 ms) of the ANPs is nearly 400-fold the lifetime of the 3F4 state of Tm3+. However, the PL lifetime of Tm3+ 3F4 state is normally shorter than 100 μs due to the serious non-radiative relaxation process or cross-relaxation between the neighbouring Tm^{3+} ions. Please check it.

Our response: This is an important point (and we wonder, from the context, if the question means to refer to $^3H_4$?). The PL lifetime of the Tm^{3+} $^3F_4$ manifold has been reported to be as long as 12 ms [Villanueva-Delgado, Pedro, et al., Phys.Chem.Chem.Phys., 18, 27396 (2016)]. This long lifetime is physically reasonable since the non-radiative relaxation rate is negligible due to the large energy gap (~15 phonons; also, surface quenching is minimized by thick shells) between the $^3F_4$ manifolds and the next highest level (the ground state). There is no cross relaxation from the $^3F_4$ manifold as it is the lowest lying excited state of Tm^{3+}.

When calculating the 400-fold difference, we used a PL lifetime of Tm^{3+} $^3F_4$ of ~1.5 ms calculated using the radiative relaxation rate and non-radiative relaxation rates derived from the DRE model.

Reviewer comment: 5. Fig. 3c: How did the authors calculate the QYs of ANPs? The details should be provided in the Supplementary Materials.

Our reply: We agree there should be more detail here and have added the description of QY calculation to the SI.

Changes to the manuscript: "Theoretical quantum yield (QY) for the $^3H_4 \rightarrow {}^3H_6$ transition (800 nm) can be calculated by using the results from the DRE simulation. The equation is expressed as:

$$QY = \frac{\#\ photons\ emitted}{\#\ photons\ absorbed} = \frac{(1-b_{32})W_3^R n_3}{\sigma^{GSA}\frac{I_p}{h\upsilon}n_1+\sigma^{ESA}\frac{I_p}{h\upsilon}n_2}$$ "

Reviewer comment: 6. The authors are suggested to supplement a table which compares the PASSI with other existing super-resolution bioimaging techniques (e. g., super-resolution stimulated emission depletion microscopy, nonlinear structured illumination microscopy, and near-infrared emission saturation nanoscopy) based on lanthanide nanoprobes or other luminescent materials. Comments on the advantages and limitations of these super-resolution bioimaging techniques are also helpful.

Our reply: We thank the referee for his insightful suggestion and have added to the SI a new table with comparisons of superresolution techniques (Table S11), which is closely adapted from a recent review of superresolution techniques (*Nature Cell Biology* 21, 72 (2019)). We also note that we are fortunate in that there have been several excellent recent reviews on this more general topic (though obviously without considering PASSI, which is now included in our new Table S11). These cover Prof. Chen's questions in far greater detail than we could provide in a single table, and thus we have also cited these in the SI table.

Changes to the manuscript: Following the Prof. Chen's suggestion, we have added a new table to the SI (Table S11; see below)

Table S11. Overview of super-resolution microscopy techniques including PASSI. Adapted from Schermelleh, *et al.*, Nature Cell Biology 21, 72 (2019).

Table S11. Overview of super-resolution microscopy techniques including PASSI. Adapted from Schermelleh, *et al.*, Nature Cell Biology 21, 72 (2019). **Method**		**Principle: detector**	**3D res. /stack**	**2-color/ multi-color**	**Live cell**	**Ease of use**	**Costs**	**Sample prep.**	**Thick>20 µm**	**Localization or Resolution Improvement**	**No additional computation / post-processing requirements**	**Refs.**
SR-SIM	Re-scan	Single-point scanning; camera	-/√	√/√	√	Easy	$	Easy	√	Low	-	38
	Airyscan	Single-point scanning: Photo-detector array	√/√	√/√	√	Easy	$$	Easy	√	Low	-	39-41
	iSIM	Multi-point scanning; camera	√/√	√/√	√	Easy	$$	Easy	√	Low	-	41,42
	Interference-based 2D/3D SIM	Wide-field (TIRF); camera	√/√	√/√	√	Moderate	$$$	Moderate	-	Moderate	-	43-46
STED		Point scanning; Photo-detector	√/√	√/-	-/√	Moderate	$$$/$	Easy	√	High	√	47
RESOLFT		STED, SIM	√/-	-/-	√	Moderate	$$$	Difficult	-	High	√	46,48,49
SMLM		Wide-field, TIRF, HILO; camera	√/-	√/-	-	Moderate	$$	Difficult	-	High	-	50,51
SOFI/SRRF		Algorithm	√	√/-	√	Moderate	$	Moderate	-	Moderate	-	52,53
LLS		Light-sheet and SIM; camera	√	√/-	√	Difficult	$$$	Moderate	√	Low	√	54
ExM		Sample prep. kit	√	√/√	-	Easy	$-$$	Moderate	√	High	√	55-57
PASSI/uSEE		Point scanning; Photo-detector/ Multi-point scanning; camera	√/√	-/-	√(?)	Easy	$	Easy	√	High	√	32,34, This work

$: low cost, $$: Moderate cost, $$$: High cost, ✓: yes/possible, SR-SIM: super-resolution structured illumination microscopy, iSIM: instant structured illumination microscopy, STED: stimulated emission depletion microscopy, RESOLFT: reversible, saturable optical linear fluorescence transitions, SMLM: single-molecule localization microscopy, SOFI: super-resolution optical fluctuation imaging, SRRF: super-resolution ring correlation, LLS: lattice

light sheet, ExM: expansion microscopy, PASSI: photon avalanche single beam super-resolution imaging, uSEE: super-linear excitation-emission

Reviewer comment: 7. Some typos or grammar errors should be checked carefully. For example, line 219: (Fig. S9, 10;); Fig. S2: Tm3; page 9 of the Supplementary Materials: “3H5” should be “3H4”.

Xueyuan Chen

Our reply: We thank the Prof. Chen for catching these mistakes; we have corrected them and some others found by us and the other Referees during the revision process.

Referee #3

Reviewer Comment: The authors of the manuscript "Giant nonlinear optical responses from photon avalanching nanoparticles" describe their results on photon avalanche (PA) upconversion (UC) observed in Tm3+ doped NaYF4 nanoparticles and discuss potential applications of PA for super-resolution microscopy. The observed optical phenomena represent all features of PA including sharp threshold in optical pump intensity and critical slowdown of the fluorescence buildup at the threshold. Due to high non-linearity of the PA, the authors could demonstrate significantly improved spatial localization of individual nanoparticles.

While the results presented in the manuscript are of high quality and certainly worth publication. However, I doubt the sufficient novelty to qualify as breakthrough.

PAUC in rare-earth-based materials is known since 1979. It is based on efficient energy transfer between Ln3+ dopants closely packed in the host material once doped at sufficiently high concentration. ....If some real application of PAUC in nanoparticles was demonstrated, that would have changed the status of the work. However, the authors only demonstrate the phenomenon known for over 40 years though for nanosized material.

Our reply: We are grateful to the reviewer for their supportive comments, that our work is “high quality and certainly worth publication”, and for presenting a number of points where we can improve our manuscript.

We appreciate that PA in Ln-based materials was first observed over 40 years ago, and we in no way want to imply that we are discovering PA in our manuscript. It was our goal in the 2nd paragraph to acknowledge the importance of this historic work and to offer readers some context for our new study. To be clearer, we have revised the introduction to include a more specific statement acknowledging that PA was observed in lanthanide materials over 40 years ago.

Changes to the manuscript: We have revised the sentence in the introduction to read: “PA was first observed over 40 years ago in Pr^{3+}-doped bulk crystals, which exhibited a sudden increase in upconverted luminescence when excited beyond a critical pump laser intensity $(I_P)^3$”

Reviewer Comment: Since this energy transfer depends on the very local, less than a nanometer, spacing between the dopants, there is no conceptual difference between PAUC in bulk and in nanosized material.

Our reply: We certainly agree that the critical energy transfer involved in PA relies on close spacing between Ln ions. But we believe this statement is at odds with the most fundamental concept of nanoscience: materials below 100 nm take on unique properties, and these present both opportunities and challenges. For PA within nanoscale materials, this has been a challenge that has not, until now, been demonstrated as in our manuscript.

Energy losses and confinement imparted by nanoparticle surfaces (and manipulated in nanoscale heterostructures) modify this photophysics relative to bulk materials, often in dramatic ways (see for example Zhao, *et al*., Nature Nanotech. 8, 729 (2013), as well as refs. [34-36] in the manuscript). These are the challenges and opportunities in designing unique nanomaterials, distinguishing them from bulk materials.

In terms of applications, nanoscale materials open a large range of possibilities. Bioimaging probes must have comparable dimensions as the cellular components that the probes target (typically, 30 nm or smaller) in order to have compatibility with living systems. Larger probes attached to cellular components may inhibit their function (e.g., binding, catalysis), retard diffusion or cellular trafficking, have limited cellular uptake or poor pharmacokinetics, and have limited access to confined spaces such as in synapses and pores (see, for example: *Nature* 2010, 467, 600; *Nat. Biotechnol*. 2007, 25, 1165; *ACS Nano* 2017, 11, 6773). Probe size is particularly important for super-resolution imaging: attaching a >100 nm probe to a biomolecule of interest is counter-productive for high-resolution imaging because doing so can introduce >100 nm of uncertainty to the location of that biomolecule, offsetting any gains in optical resolution. In contrast, the ANPs in our study are ideal in several respects for super-resolution imaging because they are comparable in size to that of commonly used primary + secondary Ab staining methods (as each Ab is ca. 15 nm in length).

Reviewer Comment: If some real application of PAUC in nanoparticles was demonstrated, that would have changed the status of the work.

Our reply: We agree, and this is the purpose of Fig. 4 and its associated discussion, where these new avalanching nanoparticles are shown to enable real-time sub-70nm superresolution imaging using only a simple technique based on scanning confocal microscopy, before any calculations. With photon localization calculations, the localization accuracy is just 2 nm. this approach can immediately impact real imaging experiments and applications, and we answer the reviewer's specific questions about it below.

Changes to the manuscript: We have added a new Table S11, which compares ANP-enabled superresolution to other existing techniques (see table above in response to Referee 2, comment 6).

Reviewer Comment: Apart from this major concern, I would like to mention that the manuscript contains some unsupported and sometimes even false statements. Let us start from the abstract. The authors write: "However, the photon avalanching (PA) mechanism underlying these optical innovations has been observed only in bulk materials and aggregates6,7, and typically at cryogenic

temperatures5-8". At the same time, they reference the work [5], in which there exists Table 2 showing that 45% of the PAUC materials investigated by the year 1999 exhibit PA at room temperature. The same claim is later repeated in the main text: " PA has been observed mostly at cryogenic temperatures5-8, with a few room-temperature exceptions6,7,22-25". 45% is not a few exceptions.

Our reply: Fair point, and we have removed all of these statements about cryogenic temperature.

Changes to the manuscript: We have removed statements related to cryogenic temperature from the Abstract: "However, the photon avalanching (PA) mechanism underlying these optical innovations has been observed only in bulk materials and aggregates[6,7], limiting its utility and impact in many applications."

as well as the Introduction: "Its discovery quickly led to the development of other lanthanide-based bulk PA materials, utilized e.g. in efficient upconverted lasers[4-6,16], and its unique properties continue to spark interest over diverse fields[6,7]."

Further, we have included additional references and temperature data where available in our new Table S10 summarizing previous energy looping and related effects in Ln-based nanomaterials.

Reviewer Comment: The authors write: "In conclusion, we report a new class of steeply nonlinear nanomaterials, realizing PA in engineered nanocrystals at room temperature with continuous wave pumping." They do not report a new class of materials, this is one material in terms of dopant-host combination.

Our reply: We agree "class" is overreach and have removed it.

Changes to the manuscript: The revised first sentence of the conclusion now reads: "In conclusion, we report steeply nonlinear nanomaterials, realizing photon avalanching in engineered nanocrystals at room temperature with continuous wave pumping."

Reviewer Comment: The authors write: "these results immediately open new applications in ultrasensitive IR photon detection". I strongly doubt that PA would ever be able to compete with superconducting light detectors that can work up to 5-6um in wavelength, are more or less wavelength-independent, and have 90+% quantum efficiency.

Our reply: We also agree that these ANPs will not compete with the efficiency or wavelength response of superconducting light detectors and have removed this potential application.

Changes to the manuscript: We have revised that sentence to now read: "…these results can open new applications in local environmental, optical, and chemical reporting, and in superresolution imaging", which we feel are applications that can directly benefit from the steep nonlinear response of the nanoparticles.

We have also revised the last sentence of the abstract, which now reads: "The low PA threshold and exceptional photostability of ANPs also suggest their utility in a diverse array of applications[7] including sub-wavelength imaging[7,11,12] and optical and environmental sensing[13-15]"

Reviewer Comment: The authors write: " More generally, by moving beyond the standard mechanisms, PA can not only enhance upconverting brightness and efficiency, but also offers unprecedented opportunities for technological innovation, since extremely nonlinear materials with controllable properties are essential for new electronic, photonic, and energy management technologies needed to address the growing societal demands for rapid and energy efficient sensing, information processing and transduction." The mechanism is pretty standard and is described as a second order phase transition (see Ref.[26] of the manuscript). Furthermore, the statement sounds as if the PA was capabale of solving all technological problems without giving a single example of "unprecedented opportunities for technological innovation".

Our reply: We appreciate the referee's point about avoiding overstatement and have removed the sentence from the manuscript.

Changes to the manuscript: The new concluding paragraph, with this language now removed, reads:

"In conclusion, we report steeply nonlinear nanomaterials, realizing photon avalanching in engineered nanocrystals at room temperature with continuous wave pumping. We observe that core-shell architectures doped with only Tm^{3+} ions exhibit avalanching behavior for Tm^{3+} concentrations ≥8%, and that the PA excitation threshold intensity is fully determined by the $^3F_4$ intermediate state lifetime at higher concentrations. Further, we show that PA is achieved for excitation in the 1400 – 1470 nm range in addition to 1064 nm. Along with emission intensities that scale nonlinearly with pump intensity up to the 26^{th} power – enabling sub-70 nm SCM imaging resolution and <2 nm photon localization – these results can open new applications in local environmental, optical, and chemical reporting, and in superresolution imaging."

Reviewer Comment: Coming to the second part of the manuscript, namely, super-resolution imaging with PAUC nanoparticles, I would like to raise several concerns. First of all, imaging nanoparticles dried on the glass slide and that of the same nanoparticles in a more complex environment are very much different. For immobilized nanoparticles it is easy to adjust the pump intensity very close to the PA threshold and, therefore, obtain high localization. Once they are in solution, the rotation of the nanoparticle will lead to turning of the Ln3+ ESA dipole with respect to pump polarization and, therefore, will make imaging close to PA threshold impossible.

Our reply: We appreciate these concerns, and we have carefully considered them in light of both the requirements for bioimaging and the response to ANPs under polarized excitation. In our experience with superresolution imaging and our close reading of the literature, the vast majority of subdiffraction bioimaging is carried out on fixed tissue, with fully immobilized probes, and this is essentially identical to probes immobilized on glass. For live-cell superresolution imaging (typically, tracking of membrane proteins, proteins moving along the cytoskeleton, or interacting with organelles), we expect motion within the plane of the membrane but little or no rotation of the probe, which must be stably conjugated to a biomolecule of interest. There may be instances of superresolution bioimaging in which the probes rotate (such as tracking the motions of intracellular proteins not affixed to the cytoskeleton or an organelle), but these would be unusual and likely better handled with GFP-based probes (e.g., using PALM), which can be expressed as chimeras to the protein of interest.

Even if our avalanche nanoparticles were to rotate during imaging, they are unlikely to show any significant dependence on the polarization of the pump radiation. While polarized emission has been observed for larger microcrystals with dimensions comparable or greater than the wavelength of light, this polarization anisotropy has be attributed to optical birefringence, optical modes associated with the larger crystal geometry, or the polarization response of a coupled antenna. These effects are not relevant to the much smaller hexagonal-phase nanoparticles used in our work, so the only possible polarization responses might be those intrinsic to the emission of individual Tm^{3+} ions. The crystal field can impart some polarization dependence (symmetry breaking can add some dipole character to the transitions), though smaller than that from a pure dipole. The S_6 symmetry of the Ln^{3+} site in Ln-doped beta-phase $NaYF_4$ suggests that there would be no permanent dipole surrounding the Tm^{3+} emitters (see: "Optical Properties of Nd:NaYF4 and Ho:NaYF4," in Advanced Solid State Lasers, Vol. 5 of OSA Proceedings Series (1989), paper CC7) in our ANPs, and thus little polarization dependence. And unlike larger crystals, which tend to grow into prolate structures, smaller nanocrystals are closer to spherical in shape, with heterogeneous strain gradients, lattice distortions, and surface reconstruction. All of these phenomena may further reduce polarization anisotropy to levels below other sources of noise and heterogeneity.

This lack of polarization dependence is evident in the numerous reports detailing the imaging of small single Ln-doped UCNPs. Near-uniform intensities have been reported from single nanoparticles from a given batch in many (or all) single UCNP studies (e.g., see *Nat Commun.* 2018, 9, 3082; *PNAS* 2009, 106, 10917; *Adv. Mater*. 2009, 21, 4467; *Nat. Nanotech*. 2014, 9, 300), despite linearly polarized excitation and random orientation of each particle on the substrate, as there is no preferred particle orientation on the substrate in these experiments. Individual nanoparticles in these studies are identified using independent methods, and small variations in particle-to-particle intensity fall within expectations based on differences in particle size.

Reviewer Comment: Second point: imaging of PAUC nanoparticles is intrinsically based on scanning the excitation beam through the emitting species, similar to confocal or STED microscopy. Thus, the image is supposed to be collected pixel-by-pixel with up to 600ms per pixel due to critical slowdown. Furthermore, the pixel size should be smaller than the expected resolution of the image, i.e. 65nm. Thus, in 1 second the authors would collect the fluorescence of two pixels, say, 30nm apart. In order to scan through the size of the focal spot of the excitation laser (300nm), 50 seconds are required. This is the minimal size of the area of a single beam in a multi-point approach. 50 seconds per frame differs drastically from the claimed rate of 1 frame/second.

Our reply: We appreciate this comment by the referee, as it offers us the opportunity to clarify the manuscript about the optimal intensity for use in ANP imaging. As discussed in more detail in ref. [7], optimal resolution is achieved when imaging with intensities somewhat beyond threshold – at an intensity near the top of the steep part of the response curve, typically 1.1-1.3 times the threshold intensity. This allows us to exploit the steepest nonlinear response of the ANPs. In SCM, for a point emitter with a nonlinear response, the theoretical limit for the FWHM of an imaged spot is given by:

$$\text{FWHM} = \lambda/(2\ \text{N.A.}\ \boldsymbol{s}^{1/2})$$

in the Gaussian optics approximation, where the dependence on the nonlinear order ***s*** can be seen directly. The resolution is best when the nonlinear order ***s*** is largest, which corresponds to the steepest part of the response curve.

At the PASSI optimal intensity, the rise time is not 600 ms (which is the rise time at threshold), but is approximately 200 ms. This immediately reduces the 50 second frame rate calculated by the referee to ~16.7 s – a 3x improvement, but still longer than a frame rate on the order of a second.

The other important factor is that, in the scanning scenario accurately described by the referee, the particle is partially illuminated by the sides of the excitation spot even before the spot passes directly over it. In this case, the partial illumination effectively "seeds" the avalanche rise-time kinetics by initiating some absorption events, significantly reducing the rise-times when the excitation spot moves over the ANP. Thus, pixel dwell times of only ~50 ms or less can be used without sacrificing signal, resulting in frame rates of ~4 s or less.

Changes to the manuscript: We have performed experiments verifying this "seed" rise-time acceleration concept (note that in image scans, the ANP will be seeded by multiple pixels before the excitation spot is centered on it). These plots and associated discussion have now been added to the Supplemental Material as new Fig. S11 (copied below) to better explain the concepts and photophysics that lead to the faster frame rates.

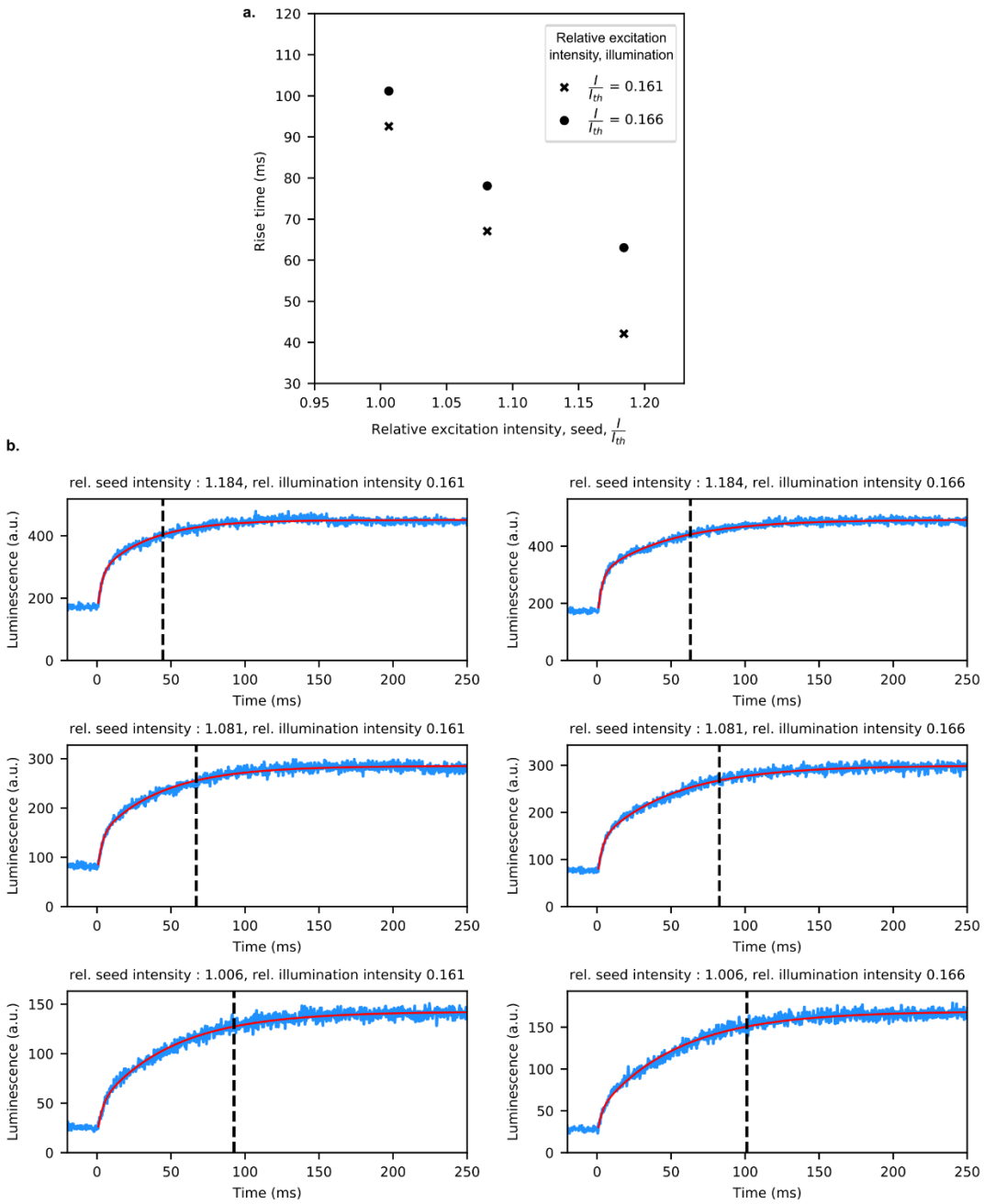

Fig. S11. Reduction of risetime with seed excitation. **a,** Measured rise time vs. seed excitation intensity (intensities normalized to threshold intensity I_{th}). Seed excitation is pre-irradiation onto the sample before the illumination excitation. Rise time is measured with continuous seed excitation and oscillating illumination excitation (square wave). **b**, Time-resolved luminescence depending on seed and illumination excitation intensities. Red curves are bi-exponential fitting curves and black dashed lines indicate 90% rise time.

While the measurements imply that rates could be faster, we believe it is best to be conservative in our frame rate estimation and have updated the main text to now read: “Realizing that the longer rise times might limit scan rates[51], we also calculated a multi-point excitation scheme (Figs.

S11,12,13), which suggests possible scan rates of approximately 4 seconds or less per frame are achievable and reasonable using multi-point PASSI"

We have updated the main text to better clarify the optimal excitation intensity for PASSI to now read: "We performed single-ANP imaging, measuring a PASSI image spot of ≤75 nm average FWHM when excited at 1064 nm at the optimal pump intensity for PASSI, which corresponds to emission intensity at the top of the steep section of the response curve [7] (see Methods for imaging details)."

Also, we have added the above equation to the main text, as well as a reference for this equation:

$$"FWHM = \lambda/(2 \cdot NA \cdot \sqrt{s})$$

in the Gaussian optics approximation[49] (where NA is numerical aperture and λ is wavelength)."

New Ref. 49: T.R. Corle and G.S. Kino, *Confocal Scanning Optical Microscopy and Related Imaging Systems* (Academic Press, 1996).

Reviewer Comment: The third point: in order to obtain the localization accuracy of 2 nm, the authors have to work at the threshold and reduce their signal 10000 times (quote: "Finally, we note that in characterizing this PA system, we measure ~500-10,000-fold increases in emission intensity when pump intensity is increased from threshold to twice the threshold value"). 10000 times more signal means 100 time better SNR and, therefore, 100 better localization. Is PA really the better method to localise particles in light of these numbers

Our reply: We appreciate the question, as indeed the localization accuracy depends on SNR as the referee notes. In light of the response to the previous comment where we clarified the optimal pump intensity used for imaging, we hope it is now clear that the signal at these conditions is not 10000x weaker than for higher pump intensities, but only ~10x smaller. This is illustrated in Fig. S10, where we have experimentally quantified this difference.

Because photon localization accuracy is proportional to σ/SNR (σ is the Gaussian width of the imaged spot), the reduction in image spot size at the somewhat lower pump intensity more than makes up for the decrease in SNR. Experimentally, we find that photon localization is most accurate (< 2 nm) at the optimal pump intensity for PASSI, but only increases slightly for higher pump intensities because of the tradeoff noted by the referee.

Changes to the manuscript: We have updated Fig. S10 (Fig. S8 in the previous version) to explicitly state both the threshold intensity and the optimal intensity for superresolution imaging, as the last sentence of the figure legend:

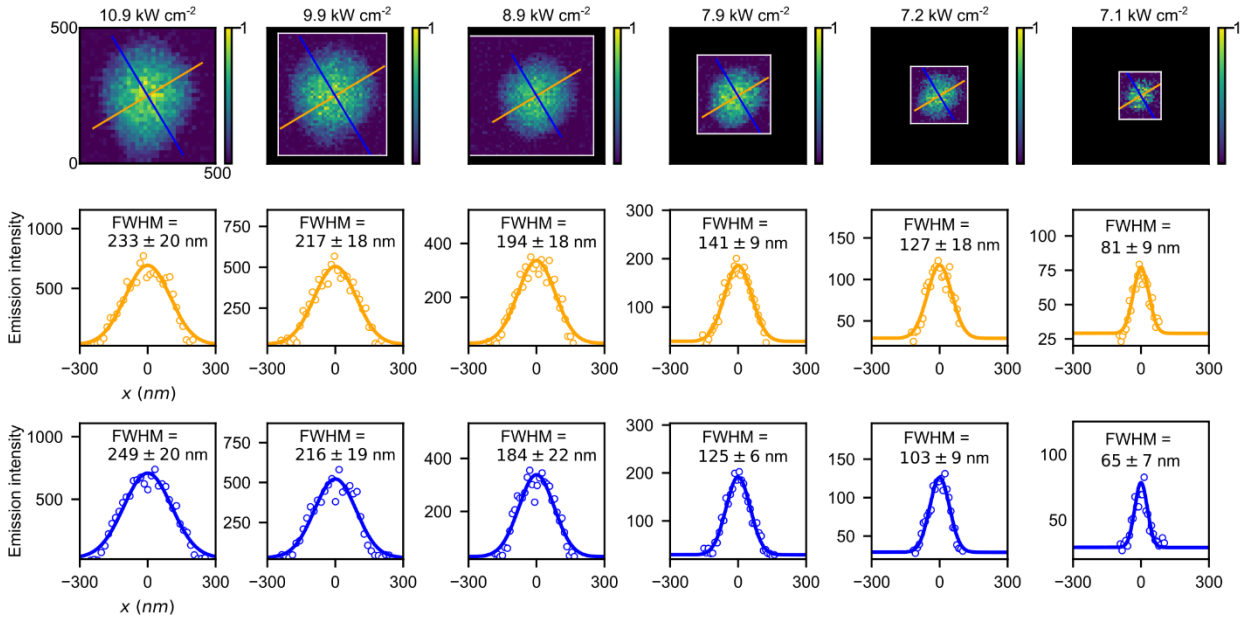

Fig. S10. 2D sub-diffraction resolution imaging of a single 8% Tm^{3+} core/shell ANPs. Data points extracted along the linecuts are shown as circles the same color as linecuts. Data are fitted as Gaussian lineshapes. FWHM values and standard deviations of fitting are denoted in the plots. Narrowest FWHM is achieved with 7.1 kW cm^{-2} excitation intensity (right panels) and threshold value is 6.4 kW cm^{-2} (see Table S3).

We also now list the threshold values in new Table S3 underneath Fig. S3, and have clarified the Fig. S3 legend:

Table S3. Photon avalanche threshold.

Sample No.	*Tm^{3+} concentration* (%)	*Threshold* (kW cm^{-2})
3	8	23.34
4	8	6.45
5	8	4.94
6	20	32.82
7	20	21.65
8	100	29.58

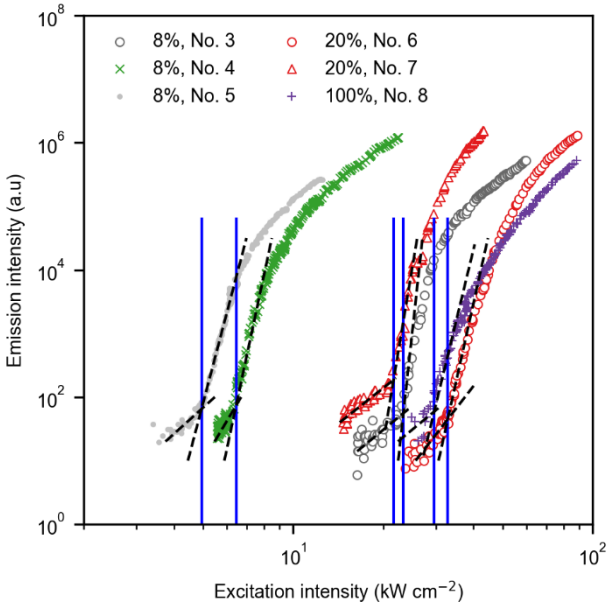

Fig. S3. Determination of photon avalanche thresholds. The threshold value reflects the change in slope of the emission intensity vs. excitation intensity curve (measurements on ensemble films). Dotted black lines are linear fits of the data points below and above threshold, where the intersection is considered the photon avalanche threshold. Percentage values are Tm^{3+} doping, and sample numbers are listed (see Table S1 for sample info). Threshold values are listed in Table S3.

As discussed above, we have now revised the text to better clarify the description of optimal imaging intensity for PASSI. Additionally, we have added an equation describing the theoretical limit for the FWHM of an imaged local emitter with a nonlinear response.

Reviewer Reports on the First Revision:

Referee #1 (Remarks to the Author):

I appreciate the careful response of the authors. The changes made in response to the comments have clarified what was needed while also mistakes have been corrected. The manuscript can be accepted in the present form and is an impressive piece of work that will have a large impact in the community.

Referee #2 (Remarks to the Author):

The authors have made an appropriate response to the referees' comments and revised the manuscript accordingly. All my concerns have been well addressed. The quality of the revised manuscript is much improved in comparison with its previous version. I have only one minor suggestion as noted below.
1. Lines 54-55 of page 2: The authors have added a sentence "the cross-relaxation process is accompanied by the emission of phonons to compensate an energy mismatch of ca. 1200 cm-1", in response to Comment #2 of Referee #1. It is inappropriate to supplement the statement here, as it lacks a background introduction about the cross-relaxation process between specific

transitions of Tm3+ ions. What does the energy mismatch refer to? Please check it.
Xueyuan Chen

Referee #3 (Remarks to the Author):

The authors added extensive data to the paper and provided several new/refined results supporting their claims. Some of the most critical points have been clarified and misleading claims were removed, i.e. the paper has improved substantially.

Author Rebuttals to First Revision:

Referees' comments:

Referee#1

I appreciate the careful response of the authors. The changes made in response to the comments have clarified what was needed while also mistakes have been corrected. The manuscript can be accepted in the present form and is an impressive piece of work that will have a large impact in the community.

Our reply: We are thankful to the reviewer for their support, and for their thoughtful comments and time in reviewing our manuscript, which we feel has notably improved its the clarity and presentation.

Referee #2 (Remarks to the Author):

The authors have made an appropriate response to the referees' comments and revised the manuscript accordingly. All my concerns have been well addressed. The quality of the revised manuscript is much improved in comparison with its previous version. I have only one minor suggestion as noted below.

1. Lines 54-55 of page 2: The authors have added a sentence "the cross-relaxation process is accompanied by the emission of phonons to compensate an energy mismatch of ca. 1200 cm-1", in response to Comment #2 of Referee #1. It is inappropriate to supplement the statement here, as it lacks a background introduction about the cross-relaxation process between specific transitions of Tm3+ ions. What does the energy mismatch refer to? Please check it.

Xueyuan Chen

Our reply: We very much appreciate Professor Chen's praise of our work as well as his careful reading and helpful comments.

Regarding the suggestion for lines 54-55: This is an excellent point, and we agree that the detailed nature of this statement is out of place in the introductory discussion of general PA. We have now moved the sentence out of the introduction; instead it can be found in the Methods discussion of PA mechanism in our ANPs, where we note:

"This mechanism amplifies the population of excited states, such as the 800-nm-emitting Tm^{3+} $^3H_4$ level (Fig. 1c), through a positive feedback loop of ESA from an intermediate state ($^3F_4$) followed by cross-relaxation (an energy transfer process) back down to the same intermediate state while promoting a second ground-state Tm^{3+} ion up to its intermediate state (note that the cross-relaxation process is accompanied by the emission of phonons to compensate an energy mismatch of ca. 1200 cm^{-1})."

Referee #3

The authors added extensive data to the paper and provided several new/refined results supporting

their claims. Some of the most critical points have been clarified and misleading claims were removed, i.e. the paper has improved substantially .

Our reply: We are grateful to the reviewer for their comments and suggestions, which have resulted in marked improvements to the manuscript.